Examensarbete
TVVR 13/5006

Wave-Damping Properties of Swimming Lines

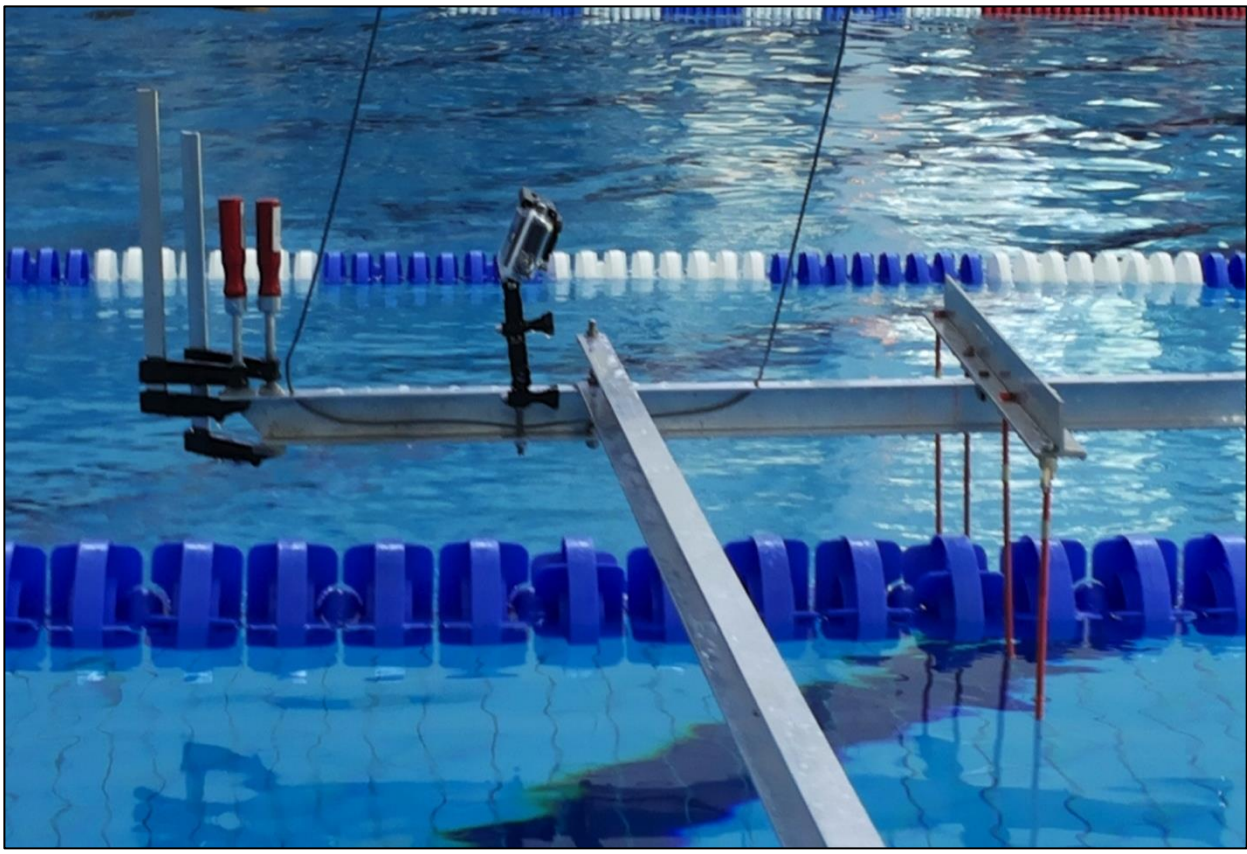

Nadim-Pierre Rizk

Division of Water Resources Engineering
Department of Building and Environmental Technology
Lund University

TABLE OF CONTENT

PREFACE

The main purposes of this study were to investigate and to quantify the efficiency of the wave damping properties of swimming lines. The major role of a swimming line is not only to separate the pool into different lanes but most importantly to damp the waves in an effective way.

Despite being a topic of increased interest, few investigations could be found concerning swimming lines, especially regarding experimental work on their hydrodynamic properties.

The first part of this thesis consists of a brief overview of hydrodynamic concepts and the forces acting on swimmers. Furthermore, some properties of the waves generated by swimmers and characteristic coefficients of the swimming lines (transmission and damping coefficients) are defined.

The second part is a complete description of the experimental procedure employed to analyse the efficiency of the swimming lines. It includes explanations about the setup, the cases investigated, the image analysis, and some explanation of the analysis performed.

In the last part, the results from the data analysis are presented and discussed. The influence of each parameter is studied and analysed in detail regarding the properties of the swimmer, such as the speed or stroke style, and the characteristics of the waves generated by the swimmer, such as the period and height. Also, the effects of the swimming lines on the waves are investigated, including the transmission coefficient, the damping coefficient, type of swimming line, and the tension in the wire holding the line.

Some general principles were derived from all these observations and results. The main conclusions of this thesis were:

- The damping efficiency of the swimming line increases linearly with the diameter (over the range studied).
- The damping efficiency of swimming lines increases considerably for swimmers at high velocities and for waves with large heights.
- Further experiments should be pursued on a wider scale with some technical modifications in order to confirm the results obtained in this study.

ACKNOWLEDGMENTS

Writing the present thesis would not have been possible without the continuous support of several individuals and organizations.

I would like to express my gratitude towards my coordinator, Professor Magnus Larson for giving me the opportunity to pursue this project. His supervision and guidance were crucial in the completion of this thesis.

Many thanks also go to Malmsten Company for believing in this project, and for providing the support needed in terms of swimming lines.

Furthermore, I would like to acknowledge with much gratitude the vital role of the staff of SK Poseidon club at Högevallsbadet swimming pool in Lund, both the swimmers and their coach Thorbjörn Holmberg.

My appreciations and thanks also go to two people in particular: Lennart Grahn from the Water Resources Department and Peter Jonsson from the Engineering Geology Department at Lund University for their inspiring ideas and their help in supplying the necessary material and equipment in order for us to conduct the research and reach our objectives.

Finally, I would also like to thank my family and friends for their constant encouragement and for some of them, for their participation in the experiments as swimmers.

1 Introduction

1.1 Background

In the increasingly professionalized world of swimming, beyond the sheer technique and fitness of swimmers, considerable effort has been put into altering and optimizing the swimmer's surroundings, most notably in terms of infrastructure and equipment.

New swimsuits and building larger or deeper swimming pools are all methods that can be used to help swimmers go faster. Similarly, the use of swimming lines is another crucial tool that can optimize one's swimming speed. We will turn our attention to the properties of these swimming lines, which ensure that swimming lanes are less turbulent by damping the waves from the swimmers, and hence enabling a swimmer to swim with the water flow and not against it.

While originally created to simply separate different lanes in a pool and to prevent swimmers from swimming in each other's lanes, swimming lines are now playing another essential role due to their wave-damping properties – a topic that has attracted little attention so far from researchers and academia. Nevertheless, in a sport where every hundredth of a second counts, controlling the wave action and thus offering a more stable swimming platform, is slowly but surely becoming a topic of increased interest in the world of swimming.

1.2 Objectives

The main objective of this thesis is to investigate the efficiency of swimming lines in damping waves generated by swimmers. Swimming lines consist of a string of floaters used to separate the different lanes in swimming pools, especially during competitions. The focus of the present study is to analyse and test the properties of swimming lines, particularly with regard to their ability to dampen waves from the swimmer, avoiding wave transmission into neighbouring lanes as well as wave reflection back into the lane of the swimmer generating the waves. More efficient swimming lines would therefore allow the swimmer to compete under the same conditions, and not be affected by the waves generated by his/her competitors.

The study will determine the characteristics of the waves generated by the swimmer and how these waves are transformed as they impinge upon the swimming line. The transmission coefficient will be calculated based on experimental data and the overall wave-damping efficiency of swimming lines will be assessed. In order to

conduct this study, swimming lines manufactured by the company Malmsten AB were employed in the different experiments carried out. The response of the swimming lines to waves generated by several swimmers swimming at different speeds while performing different types of strokes, that is, crawl, breast, backstroke, and butterfly, will also be studied.

1.3 Procedure

The study encompassed the following main parts:

A review of appropriate literature was carried out, including literature on swimming lines and waves generated by swimmers. Since the former literature is rather limited, especially with regard to the wave-damping properties, the main data in the present study will be obtained through laboratory experiments under prototype conditions in a swimming pool. The water level variation at several locations around the swimming line was recorded as swimmers passed by using different types of strokes and varying their speed. The water level was recorded using video cameras followed by image processing techniques.

The experimental data on water level variations collected during the laboratory experiments were analysed in terms of different wave properties. Using the "multiple frame per second" camera mode, each time a swimmer passed next to the prototype, a series of 30 pictures during 3 seconds was taken. Performing such analysis repeatedly provided a basis for estimating values on the transmission coefficient of the swimming lines. Such coefficient values were determined for different strokes, swimmers of different size swimming at varying speeds, as well as for two types of swimming lines.

In **the data analysis**, the influence of each parameter was studied and evaluated, whether it concerned the swimmer, such as his speed or his stroke style, the waves generated by him/her, such as the period and height, or whether it was about the swimming lines, such as the transmission coefficient, the damping coefficient, the type of swimming lines or the tension in the wire holding it.

Some **general principles were derived** from all these observations and results, and some suggestions are given for future studies and regarding the potential improvements of the current design of the swimming lines.

2 Hydrodynamics of Swimming

2.1 Basic hydrodynamic concepts

"The water is your friend [...] you don't have to fight with water, just share the same spirit as the water, and it will help you move". Alexandr Popov, a famous Russian sprinter dubbed “The Tsar” - double Olympic champion in the nineties - was describing this complex interaction between swimmers and water. Despite the rather philosophical and inspirational nature of Popov’s statement, his views overlap with a clear observation: swimmers should swim with the water and not against it, in order not to waste energy caused by a flawed coordination in the movement, a faulty technique, or wrong timing. This complex interaction between swimmers and water could be further discussed through the study of hydrodynamics of swimming and fluid dynamics on a wider scale.

Hydrodynamics can be defined as the scientific study of the motion of water, under the influence of internal and external forces, and it has been a rather popular research topic in swimming for the past three decades. However, despite the increased interest among swimming coaches, scientists, and admirers, and despite the fact that it plays a crucial role in swimming and swimmers’ performances, studies on the hydrodynamics of swimming are still scarce and limited. As the human body’s movement is so elaborate and complicated compared to all other swimming mammals, its efficiency can always be enhanced with the help of research, experiments, and the use of new technologies.

For instance, recent research (Marinho et al., 2009) have shown that even the position of one’s thumb during swimming - displayed in figure 2 -, whether it is fully abducted, partially abducted, or not abducted, can have considerable effects on the swimmer’s propulsion and speed. It was shown that at times when the angle of attack of the arm - illustrated in figure 1 - is between 0˚ and 45˚, the fully abducted position of the thumb is the most efficient, whereas when the angle of attack is 90˚ the abducted position of the thumb results in a better performance.

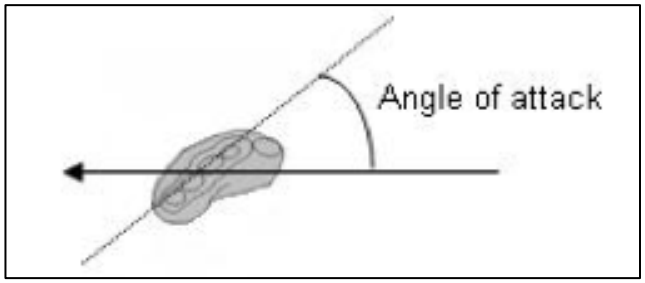

Figure 1: The angle of attack of a swimmer's hand (Schleihauf, 1979).

Figure 2: Models of the hand with different thumb positions: (from left to right) fully abducted, partially abducted, and non-abducted (Marinho *et al*., 2009).

Hence, a relatively minor detail such as one's thumb position can have a significant impact on the swimmer's speed.

Bearing in mind Marinho's research, the main aim of hydrodynamics and fluid dynamic studies in this context is to help understand the human body movement under water in a way that propels motion and decreases energy losses.

By teaching young swimmers the proper swimming techniques, they will acquire all the appropriate tools, which will allow them to swim more proficiently. As a result, their overall performance will drastically improve in the long term.

One of the most important factors in order to improve our understanding of hydrodynamics of swimming is none other than the general flow conditions, which can be laminar or turbulent. On one hand, "a laminar flow is a flow in which the water travels smoothly and rectilinearly, without any disturbance […] consisting of thin horizontal layers or laminae" (Vorontsov and Rumyantsev, 2008). Laminar flow often occurs for streamlined profiles at low velocities.

On the other hand, for a high amount of frictional and pressure forces - due to viscosity and flow separation, respectively - around the swimmer moving at high speed, the probability of turbulence occurring increases considerably, as shown in figure 3. "The turbulent flow is characterized by the random three-dimensional motion of fluid particles superimposed to the mean motion" (Naemi et al., 2010).

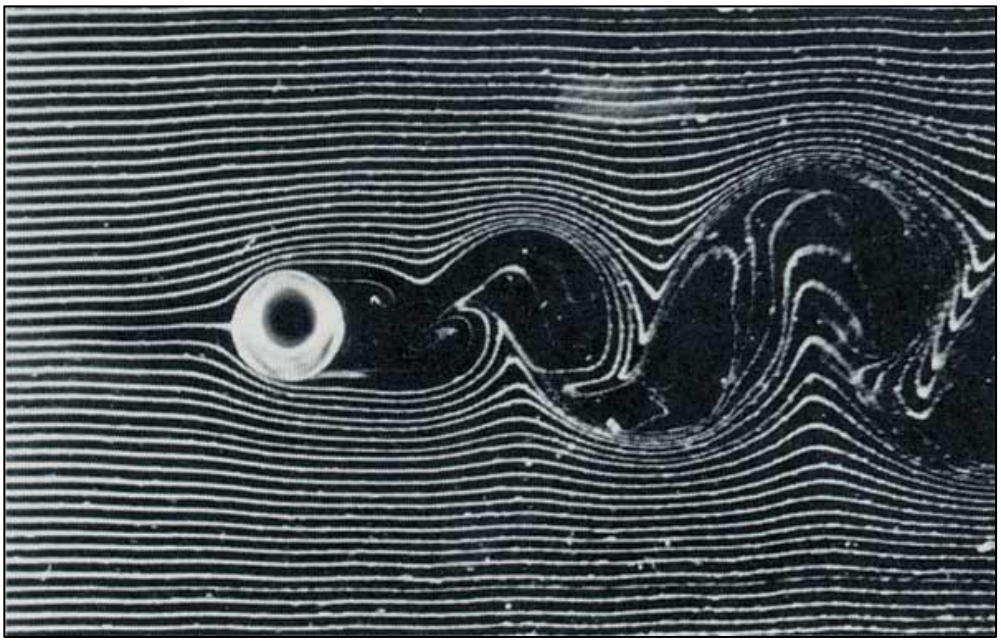

Figure 3: Turbulence in the form of vortices created behind an object in an originally laminar flow (Hill, 2012).

In order to determine whether the flow conditions are laminar or turbulent, one can refer to the Reynolds number (Re), which can be seen as the ratio between the inertial forces and the viscous forces. The Reynolds number Re is defined as:

$$\mathrm{Re} = \frac{\rho \, v \, L}{\mu} \qquad (1)$$

Where ρ: The fluid density
v: The flow velocity
L: The length of the object in the direction of the flow
μ: The coefficient of dynamic viscosity

For a smooth plate without irregularities $Re = 5.10^5$ is the transition limit between a laminar and a turbulent flow. If a swimmer swims at approximately 2.5 m/s and if we assume the limiting Re number remains the same, only the hands of a swimmer will be in a laminar flow and the rest of the body will be in a turbulent flow (Naemi *et al*., 2010). Therefore, it is crucial to consider turbulence when evaluating the drag force on the swimmer.

There are four main forces acting on a human body under water that play a significant role in swimming. Indeed, when swimming, each swimmer is subjected to his own weight, buoyancy, thrust and drag/resistance, as shown in figure 4.

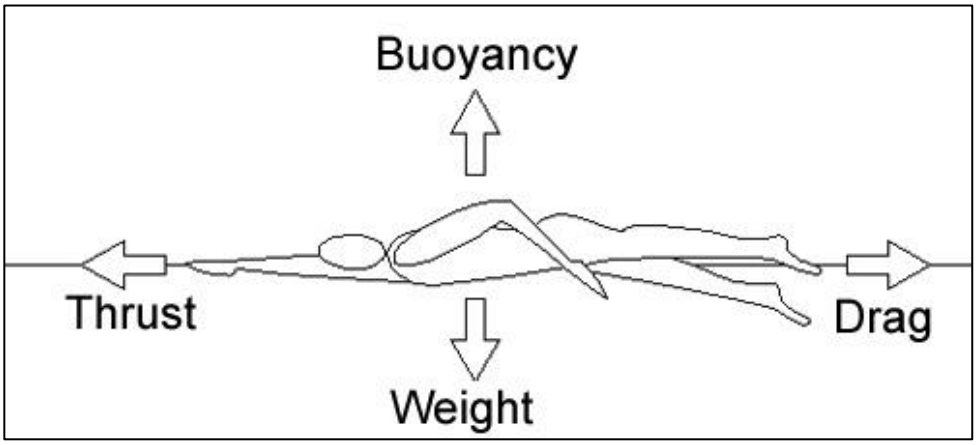

Figure 4: The four main forces acting on a swimmer (FINA, 2007).

These forces depend on several parameters such as the body surface characteristics, the depth of the swimmer below the still water surface, the swimming technique, the body size, and physical attributes of each swimmer, to name a few.

On one hand, the vertical forces, that is, buoyancy and weight will compensate each other. Archimedes Principle best describes this premise: "the buoyant force on a submerged object is equal to the weight of the fluid that is displaced by the object". (Fairman, 1996). The buoyancy force will balance the swimmer's gravity, pushing him down and displacing water from its original state.

Weight force:

$$W = mg \tag{2}$$

Where m: mass of the swimmer (kg)
g: acceleration due to gravity ($g = 9.81 m/s^2$)

Buoyancy force:

$$F = Vg\rho_f \quad (3)$$

Where V: volume of displaced water (m^3)

g: acceleration due to gravity $(g = 9.81\frac{m}{s^2})$

ρ_f: fluid density $\left(\frac{kg}{m^3}\right)$

NB: The fluid in this case is water, which has a density that varies with temperature and the water composition. The density of water is approximately $1000\frac{kg}{m^3}$.

However, it increases up to approximately $1027\frac{kg}{m^3}$ in ocean water mainly due to the higher salinity of water. This is why it requires less force to float in the ocean compared to swimming pools.

One the other hand, horizontally, the thrust propulsive force and the drag resistive force act on the swimmer. These forces will be discussed thoroughly as they are arguably the most important factors influencing a swimmer's performance.

2.2 Resistance

2.2.1 Introduction

The drag force, also known as the resistance force, acts in the opposite direction to the motion of the swimmer. This force is responsible for slowing down the swimmer. There are three main reasons or factors causing the resistance to develop.

First, water is a difficult medium to move through since its viscosity at 20˚C is around 0.001 Pa·s, which is approximately 55 times higher than air at the same temperature (Kestin, 2004). Moreover, additional resistance will be created at higher speeds because of the turbulent conditions associated with flow separation around the body. Finally, the waves generated by swimmer at the water surface, controlled by the gravitational forces, will also contribute to the drag force (Toussaint et al., 2000).

These three resistance forces, known as skin drag, pressure drag, and wave drag, respectively, generally depend on the flow conditions but they are also correlated with the body characteristics.

In the available literature, hydrodynamic resistance is often divided into two major categories and the distinction is made between the "passive resistance" and the "active resistance". "Passive resistance is that experienced by a swimmer's body during passive towing […] and when performing gliding without movement; and active resistance is that experienced by a swimmer during swimming" (Vorontsov and Rumyantsev, 2008).

One should note that both type of resistances (passive and active) include the three main components: skin drag, pressure drag, and wave drag.

2.2.2 Skin drag

The skin drag, also called frictional resistance, can be explained through the boundary layer theory. This theory is based on the following schematization: the area around the body is separated into two regions (see figure 5). The first region very close to the swimmer's body is called the boundary layer, whereas the other region is located further away from the swimmer's body where the velocity reaches the 'free stream' value.

The boundary layer is defined as the part of the flow adjacent to the body where the effect of viscosity is important (Naemi *et al*., 2010) and where the water is trying to 'stick' to the swimmer's body. Therefore, the flow velocity is zero at the surface, which is considered as the first layer of the flow, and the water travels at the same speed as the swimmer. However, at an increasing distance from the surface and due to the viscosity of water, this first layer will drag along its neighbouring layers and try to slow them down and cause a delay in the movement of the layers. This phenomenon will persist in the whole boundary layer region until the flow velocity reaches the free stream value. At this distance, the effect of viscosity becomes negligible since all layers have the same velocity. "The greater the amount of water a swimmer trails behind him, the greater is the frictional resistance" (Vorontsov and Rumyantsev, 2008).

The skin drag occurs in both passive and active swimming. Nonetheless, during active swimming, when the swimmer has a high velocity, turbulence occurs in the form of eddies in the boundary layer. This will increase the energy losses and hamper the swimmer's performance.

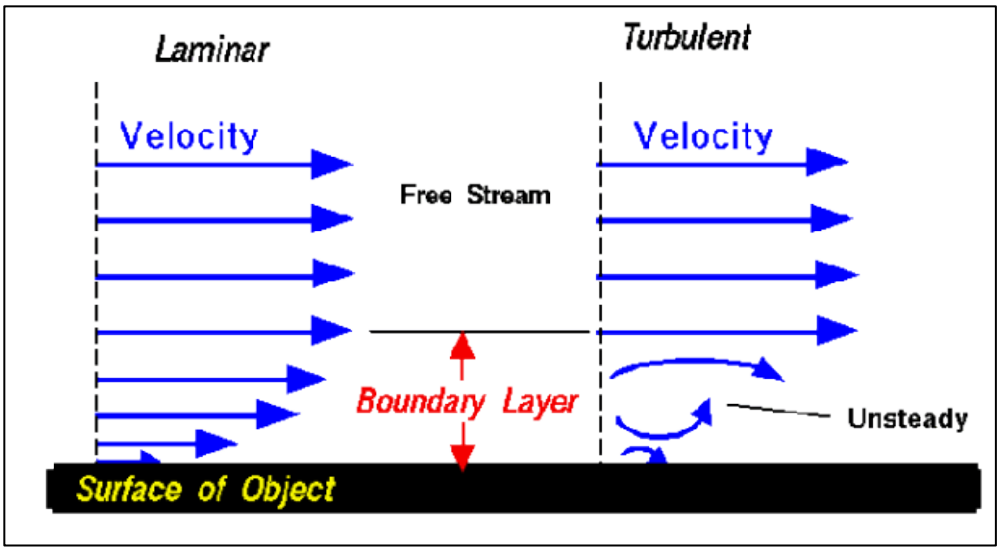

Figure 5: Boundary layer development in laminar and turbulent flow (Riyeka, 2011).

Turbulence plays a crucial role in swimming competitions since an increase of the turbulence is accompanied by an increase in the hydrodynamic resistance. Therefore, in order to avoid it, swimmers may try to have a smoother body surface by shaving or by using innovative and sophisticated swimsuits made out of ultra-thin elastic fabrics.

2.2.3 Pressure drag

The pressure drag, or form drag, can be defined as the resistance caused by the difference of pressure between the front and the rear of the swimmer's body multiplied by the projected area. The pressure acting at the front is higher than the one in the wake of the body. Because of the flow geometry, the boundary layer that initially grows along the body suddenly slows down due deceleration causing adverse pressure gradients. Consequently, there is a separation of the flow from the body which will generate eddies and turbulence in the swimmer's wake. One can therefore assume that favourable pressure gradients may maintain the flow along the body, delaying separation and the formation of eddies.

According to studies made by both Vorontsov and Rumyantsev (2008) and Toussaint *et al.* (2000) the pressure drag is the product of the pressure difference and the area to which this pressure is applied (projected area), normally expressed in term of the swimmer's speed:

$$F_P = C_D \left(\rho \frac{V^2}{2}\right) S_M \quad (4)$$

Where F_P: Pressure drag (N)
C_D: Coefficient of pressure drag
ρ: Fluid density $\left(\frac{kg}{m^3}\right)$
V: Swimming speed $\left(\frac{m}{s}\right)$
S_M: cross sectional area or projected area (m^2)

- The coefficient of pressure drag C_D takes into consideration the geometry (streamline shape; see figure 6) of the body and the general flow conditions (normally described by the Reynolds number). It is approximately between 0.05 and 0.08 for a Dolphin compared to 0.58 to 1.04 for a swimmer (Clarys, 1978). The Dolphins are considered to have streamlined bodies free of any pressures resistance centres such as the head, knees, heels, all of which drastically reduce the pressure resistance compared to human swimmers.

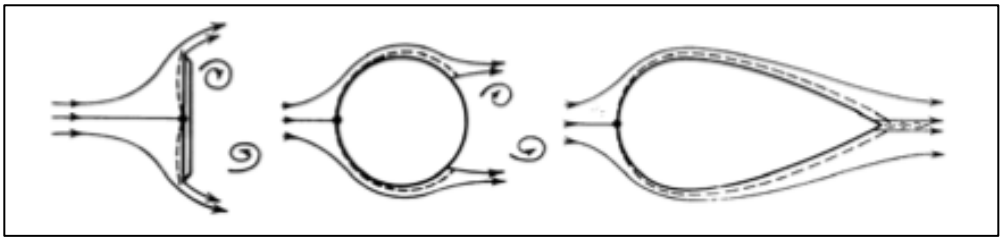

Figure 6: Three submerged objects, which are respectively not streamlined, rounded, and streamlined (Larson, 2013).

- The magnitude of the pressure drag depends on the square of the flow velocities, making the swimmer's speed the most important parameter for the drag force. Indeed, if the body is moving at slow velocities, the boundary layers will be thicker and move slower. Therefore few eddies will be formed and the skin drag will be dominant over the pressure drag. On the contrary, if the body is moving at a high velocity, the boundary layers will be thinner and move faster. Therefore, the eddies will form rapidly, the separation between the front and the 'wake' of the swimmer will occur faster, and the pressure drag will be dominant over the skin drag.

- The cross-sectional projected area S_M plays an important role as well in the pressure resistance. In order to reduce it, swimmers try to keep a streamline

position, reduce the depth of leg kick and synchronize the rotation of hips and shoulders and other body parts.

In practice, typically no separation is made between the contribution from skin friction and pressure drag when calculating the total drag force, but C_D includes both effects.

2.2.4 Wave drag

The third resistive component is called wave drag or wave-making resistance. It acts on the body when a part of it is exposed on the surface since the swimmer is "wasting" energy when generating waves instead of using it to propel him/herself through the water. This energy is lost trying to lift the waves against gravity.

Wave drag is related mainly to two important factors: the Froude number and the depth at which the body travels.

The Froude number may be defined as:

$$Fr = \frac{V}{\sqrt{Lg}} \tag{5}$$

Where g: gravity ($g = 9.81 \frac{m}{s^2}$)
L: length of the body in the direction of the flow (m)
V: Swimming speed $\left(\frac{m}{s}\right)$

It is believed that the wave drag increases with the Froude number. Hence, we can assume that taller swimmers have a slight advantage over shorter ones. Speed can be seen as a limiting factor because when a swimmer swims at a higher speed, he is increasing the probability of generating waves and wave drag resistance.

It is understood that after reaching a sufficient swimming depth, the wave drag becomes negligible and the resistance is only due to skin drag and pressure drag. In order to better understand this concept, the body can be seen as an object forcing the fluid to move at his speed. The further from the surface this "obligation" occurs, the more likely will it not affect it. This interesting depth is assumed to be approximately three times the body thickness (Naemi *et al.*, 2010). Thus, swimmers try to minimize this effect by swimming relatively deep below the surface when gliding at the start of the race, as well as at the turn.

2.3 Propulsion

The hydrodynamic propulsion is arguably one of the most complex topics in sports biomechanics. Scientists and researchers have been looking at the flow generated around the swimmer in order to try to understand the complicated mechanical movements used by a swimmer under water. These mechanisms of thrust generation depend clearly on the stroke used by the swimmer (crawl, breast, backstroke, and butterfly, among others) and the athlete's technique.

It can be seen as a simple application of the Newton's third law of action-reaction: The swimmer pushes the water backwards while the water exerts a force forward (Spathopoulos, 2013).

There are many complex theories to try to understand the propulsive forces in swimming. Among them there is the 'straight oar-like arm pull', which is mostly based on Newton's third law. Another one is the 'vortex theory' that is in general used in the analysis of swimming mammals and fish. However, the most widely accepted theory is the 'lift and lift-and-drag' (Vorontsov and Rumyantsev, 2008)

The idea is to use lift and drag in order to maximize velocity. Therefore, a swimmer should try to maximize the distance travelled each stroke by pulling back his/her hands curved for instance or by having the right angle of attack of the arm.

However, it is very hard to have a clear position on how to apply those principles. Each swimmer will develop in the end, his/her own techniques based on some natural instincts and advices given by coaches. Moreover, each stroke style requires very specific movements that differ a lot from each other. For instance, the butterfly stroke is very technical and requires a lot more coordination than the other stroke styles.

In addition to that, swimmers need to manage well his/her effort during a race. In fact, a 50 m sprint will require much more power and strength compare to a 1500m race, which will require more endurance for the muscles used for the propulsion.

3 Swimming Lines

3.1 Functioning and design

Swimming lines or lane ropes are typically used in a swimming pools for two main reasons. Their initial role was to separate the pool into different parts or aisles to improve safety in general. However, a second and more important role for competitive swimming resides in their capacity to absorb the waves or to break them. During professional swimming competitions, this attribute allows the race to be even-handed among all swimmers. On the other hand, if swimming lines are inefficient or not present, swimmers will be slowed down by the waves generated from neighbouring swimmers. In this thesis, the focus will be on the second functionality of the swimming lines. The main goal is to quantify the efficiency of these lines to reduce the waves generated by different swimmers (body size and shape), strokes (crawl, breast, back and butterfly), and speeds.

The study was made on the "competitor racing lanes" manufactured by the Swedish company Malmsten AB. This product has largely contributed to the success of the company, since it is its most exported product. It has also been used in most of the major Olympic competitions and championships for the last 35 years (see figure 7).

Figure 7: List of the sport events and competitions in which the Malmsten competitor racing lanes have been used (Malmsten, 2013).

Two different types of the competitor racing lanes were tested: the "standard" version and the "gold" version; the latter has a larger diameter and a more sophisticated design.

The competitor racing lane gold studied, displayed in figure 8, has the following characteristics:

- Diameter Ø =150mm
- Weight of 115 kg (for a swimming pool of 50m)
- Volume of 1.40m³ (for a swimming pool of 50m)

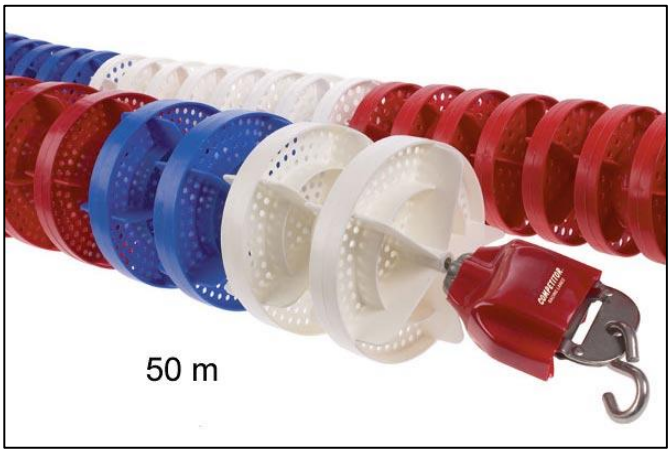

Figure 8: Competitor Racing Lane Gold: 50m, Ø =150mm (Malmsten, 2013).

The competitor racing lane standard studied, illustrated in figure 9, has the following characteristics:

- Diameter Ø =100mm
- Weight of 46 kg (for a swimming pool of 50m)
- Volume of 0.6m³ (for a swimming pool of 50m)

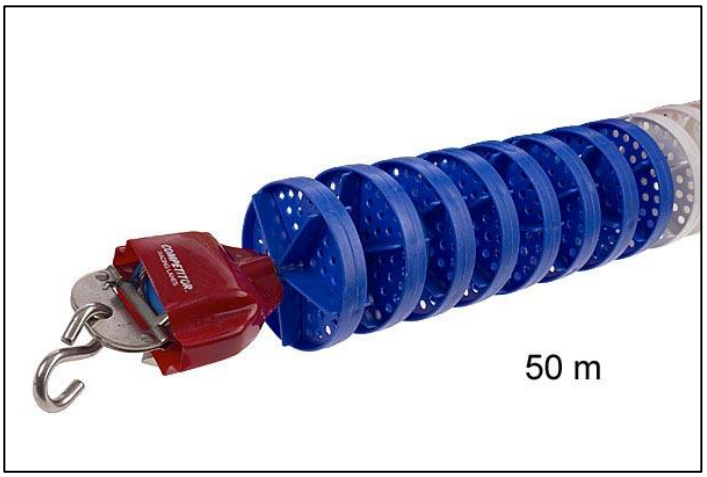

Figure 9: Competitor Racing Lane Standard: 50m, Ø =100mm (Malmsten, 2013).

3.2 Waves and hydrodynamic properties

3.2.1 Wave characteristics

According to the Oxford dictionaries[1], a wave is "a periodic disturbance of the particles of a substance which may be propagated without net movement of the particles, such as in the passage of undulating motion, heat, or sound". Water waves illustrate the propagation of energy and momentum through water. A wave 'propagates' through a medium because this phenomenon induces the transportation of energy/momentum and not physical matter or substance. Therefore, one cannot claim that a wave 'moves' through a medium.

In order to understand the hydrodynamic properties of waves generated by swimmers, some tools and definitions should be given to describe a wave. The main characteristics of a wave which are the crest, the trough, the wave height, the wave length, and the period, which are all illustrated in figure 10.

[1] http://oxforddictionaries.com/definition/english/wave

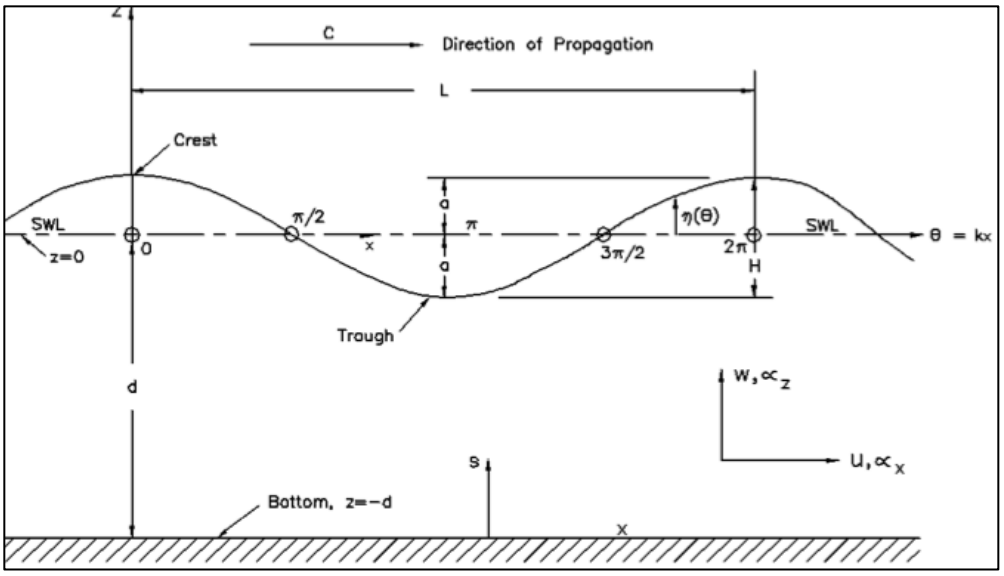

Figure 10: Illustration of wave properties (CEM, 2008).

The crest can be defined as the highest part of the wave above the still-water line, whereas the trough is the lowest part below the still water line. The vertical distance between the crest and the trough - referred to as 'H' in figure 10 - is called the wave height. In addition, the wavelength - denoted by 'L' in figure 10 - is the distance between two consecutive crests, whereas the wave period is the time needed for a wave to propagate one wavelength.

3.2.2 Hydrodynamic properties

A wave, whether it is a light, acoustic, or water wave, will react similarly when facing an obstacle. A part of it will be reflected, another part will be transmitted, and the final part will be dissipated, as shown in figure 11.

In order to quantify how a wave decomposes into these parts when it encounters the swimming lines, some characteristic coefficients were introduced. The relative contribution to the total wave from reflexion, transmission, and dissipation may be described by:

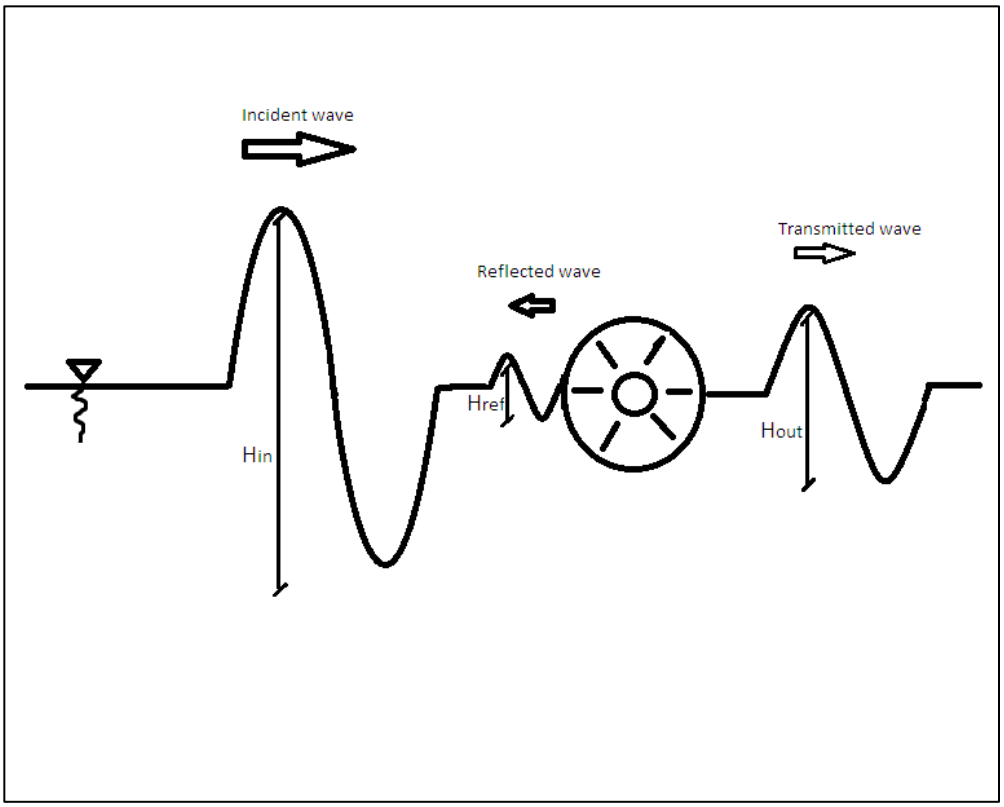

Figure 11: Transmission, reflexion, and dissipation of the wave.

$$\varepsilon = \varepsilon_r + \varepsilon_t + \varepsilon_d \approx \varepsilon_t + \varepsilon_d = 1 \quad (6)$$

Where H_{in}: Incident wave height
H_{out}: Transmitted wave height
H_{ref} : Reflected wave height

$$\varepsilon_t = \frac{H_{out}}{Hin} \text{ : Transmission coefficient} \quad (7)$$

The transmission coefficient is the ratio between the transmitted wave height over the incident wave height.

$$\varepsilon_d = \frac{H_{out} - H_{in}}{Hin} = 1 - \varepsilon_t \text{ : Damping coefficient} \quad (8)$$

The damping coefficient represents the part of the waves that have been damped or dissipated by the swimming lines.

$$\varepsilon_r = \frac{H_{ref}}{H_{in}} \approx 0 \text{ : Reflexion coefficient} \quad (9)$$

The reflexion coefficient is ratio between the wave height reflected by the swimming lines over the incident wave height (assumed negligible in the present study).

The transmission coefficient ε_t will be determined experimentally from the prototype measurements, as explained in section 4. Therefore the damping coefficient ε_d can be deduced since the reflexion coefficient ε_r is assumed to be negligible. The large number of experimental cases performed showed that the part of the wave that is reflected by the swimming line is barely observable compared to the transmitted part, which was the basis for this assumption.

The damping coefficient ε_d is one of the most intriguing parameters discussed in this study since it enables us to show and quantify how efficient the swimming line studied is for different conditions. This is why manufacturers always try to design swimming lines with a higher damping coefficient.

4 Laboratory Experiments

In this study, a system was designed and constructed in order to determine the wave-damping properties of swimming lines. The main objective behind the prototype built was to compare the waves generated by a swimmer before and after they impinged on the swimming line studied, in order to understand and quantify how efficiently these lines damp the waves.

The laboratory experiments encompassed the following five main steps:

1. Setup: building a steady prototype on which a camera is fixed to take pictures of the waves before and after damping

2. Procedure: taking a series of 30 pictures during 3 seconds every time a swimmer passes by the camera, to analyse the wave-damping properties of the swimming lines.

3. Cases investigated: The procedure is repeated for a large number of swimmers of different body shapes, swimming with several types of strokes, and at different speeds.

4. Image processing: The pictures are collected and analysed. The water level variations are manually digitized for each picture in the time series and graphs are constructed for each series showing the wave evolution in time.

5. Analysis: The properties of the waves are determined (wave height, length, and period) and analysed. The damping coefficient of the swimming line is calculated. The results for different experimental conditions are compared in order to find empirical relationships and deduce general hydrodynamic principles governing the wave damping.

4.1 Setup

4.1.1 Högevall pool

All the tests were made in Högevallsbadet swimming pool (figure 12) located in Lund, Sweden, with the help and collaboration of Thorbjörn Holmberg and the swimmers of SK Poseidon swimming club. The pool is 25m long, 5m deep, and has 8 lanes.

Figure 12: Högevallsbadet Swimming Pool (25m, 8 lanes).

4.1.2 Camera and measurement system

In order to analyse the hydrodynamics and the wave-damping properties of the swimming lines, an experimental setup had to be built. It was composed of an aluminium frame and wooden plates. This prototype was built in an attempt to film above the swimming lines the changes in the wave properties. In addition, the setup was equipped with a camera and four vertical bars with rulers to be able to quantify the observations. The camera used for recording the water surface was a GoPro HERO3 black edition (see figure 13).

Figure 13: GoPro HERO 3 black edition camera used for the measurements (Gopro, 2013).

This camera was fixed to the aluminium frame, which was stabilized on the edge of the swimming pool on one side and hanging above the swimming line on the other. This frame, shown in figure 14, consisted of three aluminium U beams with dimensions 0.6m 0.8m, and 3.5m. This frame had to fulfil two major requirements:

- It had to be extremely stable in order to avoid vibration problems and to obtain clear pictures of good quality.
- It had to be stiff enough and steady in order to overcome the deflection induced by the span of 2.45m between the border of the pool and the swimming line.

Therefore three possibilities were considered:

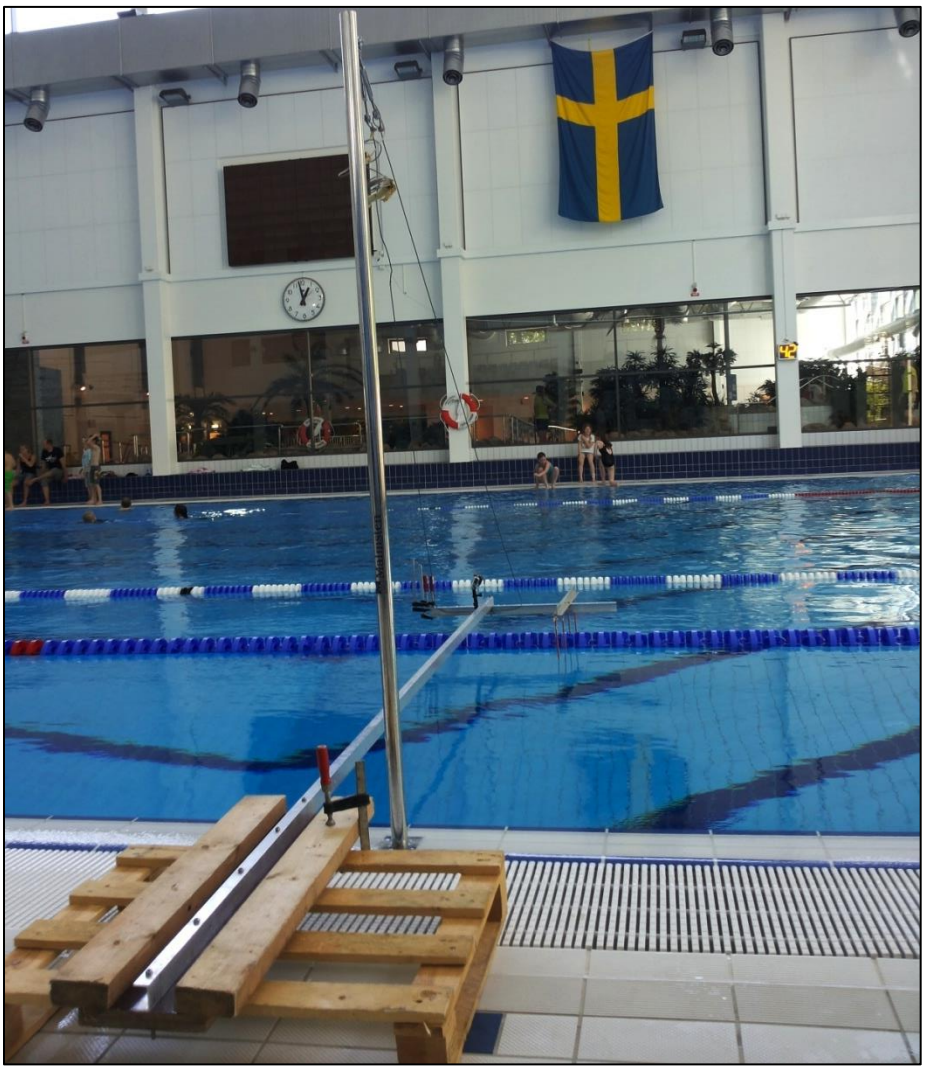

Figure 14: Prototype composed of an aluminium framework and wooden plates for the experiments.

1. A cable fixed to the ceiling of the pool, which would maintain the whole frame horizontal.

This first option was efficient but quickly appeared problematic because of the height of the ceiling and the amount of time and effort required to install it. Therefore, the first option was discarded fairly quickly.

2. A cylindrical bar made out of PVC placed in the water to support the edge of the prototype.

This solution was relatively simple and easy to implement compared to the first one. After it was implemented, the results were not satisfactory. The waves generated by the swimmer under the water caused vibrations to the PVC supporting bar. These vibrations were transmitted to the whole structure, thus giving blurred and poor quality pictures that could not be used in the subsequent analysis.

3. A stainless steel wire fixed to the extremity of the framework, which would be attached on an additional vertical bar placed on the edge of the pool.

This last option was finally adopted in order to overcome both the vibrations and the stability problems. The stainless steel wire was attached to the vertical bar on the border of the pool with the help of two shackles and two turnbuckles, which gave the prototype a certain flexibility to adjust the tension in the wire.

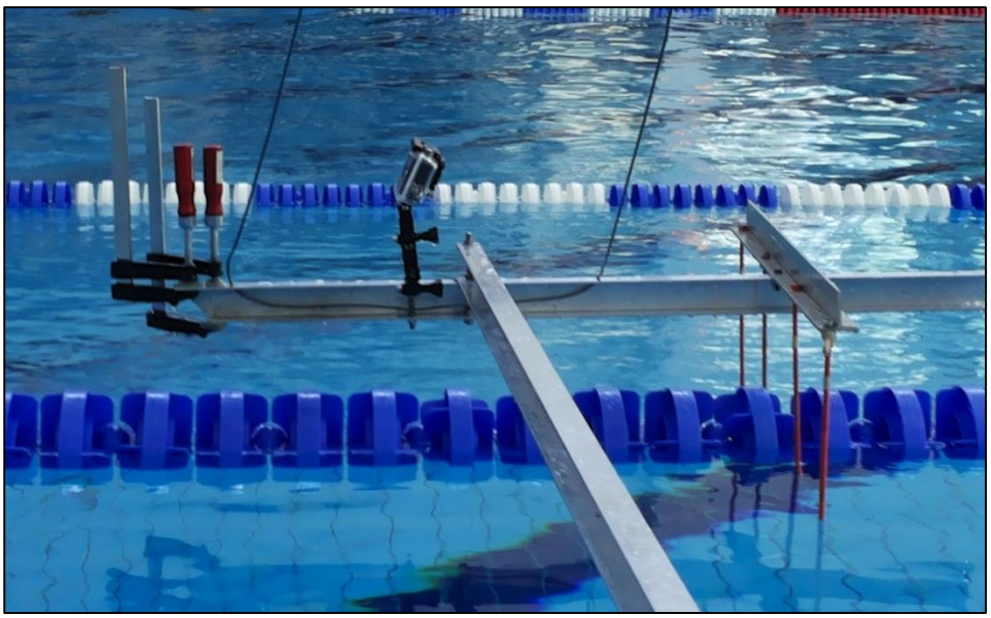

Figure 15: The edge of the prototype with the fixed camera and the red rulers.

Figure 15 shows the edge of the prototype with the Gopro HERO 3 camera fixed in the middle of the aluminium bar, which is parallel to the swimming lines. Two holes were drilled for the stainless steel wire to pass for the stability of the prototype and to remove the deflection caused by the long span of 2.25m covered.

Four bars of 25cm each were used as rulers to determine the water level on the pictures taken. These bars were painted in red in order to have a better visibility. The diameter of the bars was only 5mm so that the wave height could be determined precisely enough. Wider bars would have decreased the precision of the measurements and might have induced some vibration in the structure.

Finally, figure 15 shows two clamps to the left on the horizontal bar that were placed to compensate the weight of the rulers on the right and to have a steady, balanced setup. Consequently, it further increased the stability of the measurement system and contributed to obtain good quality pictures without any blur effect.

4.2 Procedure

During the experiments, the prototype was placed 10m away from the end of the pool to avoid unwanted effects of the reflected waves because of the turn. Swimmers were asked to swim at maximum velocity in lane number 2 while lane number 1 was kept empty as shown in figure 16.

Figure 16: Experimental procedure showing the swimmer, the measurement system, and the competitor racing lane gold.

Using the camera, tests were made employing different modes, and after several tests, it became clear that the "multiple frames per second" mode was the most adequate for the present study. Accordingly, each time a swimmer passed next to the prototype, a series of 30 pictures during 3 seconds was taken in order to capture the wave height evolution before and after the damping from the swimming line.

4.3 Cases investigated

The experiments were carried out during seven different days. Day 1 and 2 were used to adjust the setup and all the different parameters related to the testing. During day 3, 4 and 5 some amateur swimmers performed the tests, whereas during day 6 and 7 more professional swimmers from SK Poseidon club took part in the experiment. Day 5 is the day when the 'standard' version of the competitor lanes was tested whereas for all the other days, the 'gold' version was used.

The weight and the height of each swimmer were recorded in advance before the beginning of the tests. Moreover, the velocity of each swimmer was measured with a stopwatch. The type of stroke was also observed and written down for each series of 30 pictures. Swimmers were asked to swim at full speed the four main types of strokes: crawl, breast, back, and butterfly (for the advanced swimmers only).

There are approximately 120 series of 30 pictures that were taken during the different days. Only 93 series were used and a detailed description of those series can be found in the appendices at the end of the report. The 27 series left were rejected due to some practical and technical problems (interference with waves coming from other swimmers in other lanes, vibration, and bad timing in pictures).

As an example, Table 1 shows the results obtained during day 3. First, we find the basic information collected during each experimental case, such as the name of the swimmer, the type of stroke, the weight and height of the swimmer and the speed at which he/she was swimming. Second, we find the basic waves properties determined, which were obtained by the analysis of the pictures (explained in the section 4.4). Those properties are:

Ti: period of the incident wave (before hitting the swimming line)
To: period of the transmitted wave (after passing the swimming line)
Hin: Wave height of the incident wave[2]
Hout: Wave height of the transmitted wave

[2] The maximum wave height was always chosen over all others that constituted the wave time series. This choice was made as the maximum wave height can be considered the most challenging for the lines.

Series	Stroke	Name	Height (cm)	Weight (Kg)	Speed (m/s)	Ti (s)	To (s)	Hin (cm)	Hout (cm)
d3-cr-ra-1	Crawl	Raphaello	180	75	0,83	0,6	0,8	7,02	1,84
d3-cr-ra-1'[3]	Crawl	Raphaello	180	75	0,83	0,6	0,8	7,03	1,84
d3-cr-ra-2	Crawl	Raphaello	180	75	0,89	0,6	0,7	5,83	2,75
d3-cr-ra-3	Crawl	Raphaello	180	75	0,78	0,5	0,6	5,8	1,26
d3-cr-ra-4	Crawl	Raphaello	180	75	0,89	1	1	7,52	3,32

Table 1: Summary of the information collected during the experiment on day 3.

Each of the series has a name that distinguishes it clearly from the others: the first letter and number indicates the day the tests were made, going from d3 to d7. The next two letters indicate the type of stroke. The following two letters refer to the name of the swimmers. Finally, the last number indicates how many times the swimmer performed that specific stroke.

All the series of day 7, which names end by number three are those for which the tension in the cable holding the swimming lines was increased with the purpose to analyse the effects of this parameter on the swimming line. The effects of the tension will be discussed in detail in section 5.6.

4.4 Image processing

In order to derive information on the absolute location of the water level from the images, some transformation of the data recorded from the images were needed. This transformation involved three main steps:

1. Correction of the distortion: The images introduced were distorted due to the camera optics and for having placed the camera at an angle with regard to the plane in which the measuring bars were located. This was fixed using the software Photoshop CS6.

2. Wave height selection: The images were digitized and the location of the water surface was selected manually on the red rulers (bars) for each picture using a routine from Matlab called 'digitize07'.

[3] The properties of the waves for this series were calculated twice in order to perform a quality control on the procedure and image analysis.

3. Conversion from digitized into real coordinates: the corrected coordinates recorded in the image analysis were converted to real-world coordinates by using known fixed distances obtained from markings on the vertical bars.

4.4.1 Correction of the distortion

The mode selected with the camera gave pictures of 12 MP with a wide angle. Unfortunately, with such a high resolution, a small distortion of the pictures could not be avoided. However, this distortion was corrected for using the software Adobe Photoshop CS6. An example of the correction done is shown in figures 17 and 18 during 'day 6' of the tests with Michael swimming using butterfly stroke.

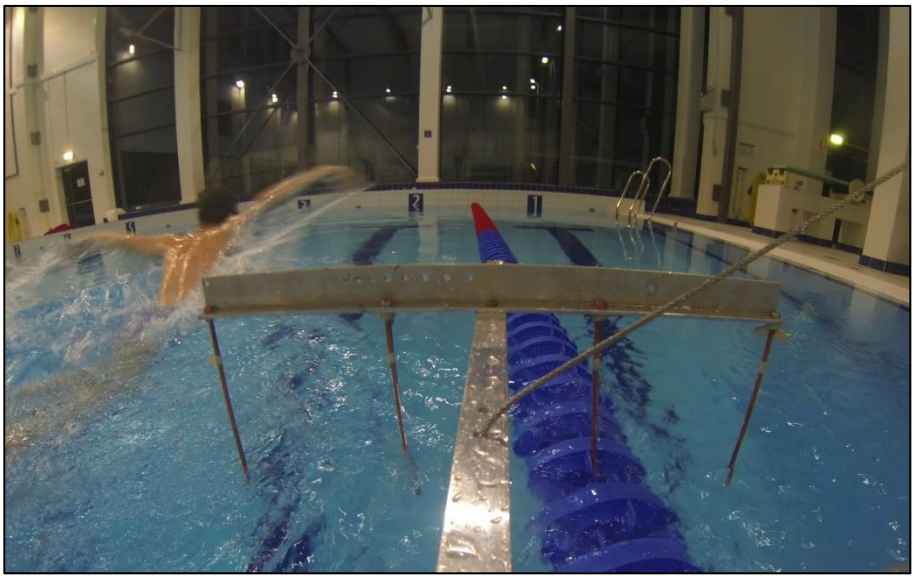

Figure 17: Original distorted picture.

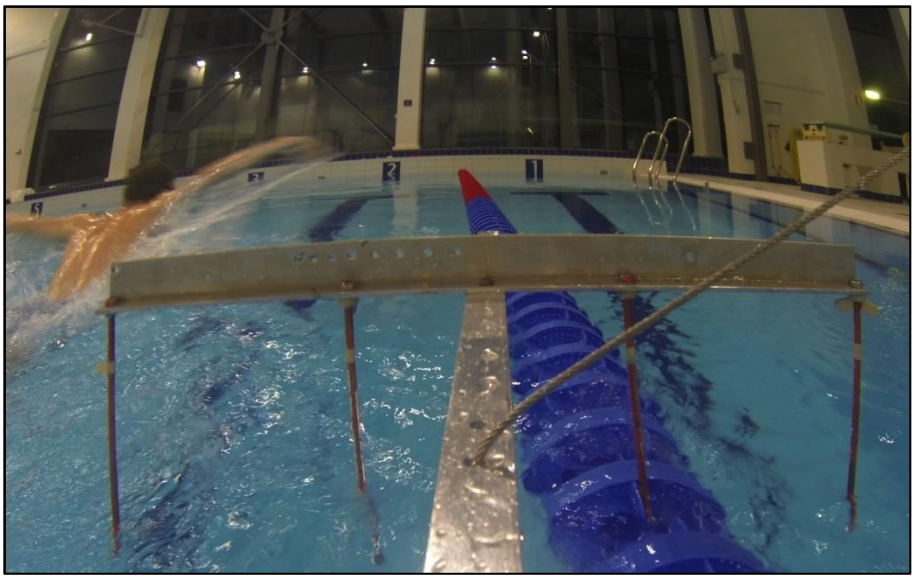

Figure 18: Final picture after correction of the distortion with Photoshop CS6.

4.4.2 Wave height selection

After correcting the distortion of the pictures, the next step consisted of selecting manually the water level position on the fixed red rulers. The selection was done for each of the 30 pictures in the series in order to obtain the water surface variation in time.

This procedure was carried out using a routine from Matlab called “digitize07” that can be found in detail in the appendices. This routine made it possible to select the points needed on the pictures - after zooming in on the area wanted - and to obtain the digitized coordinates.

Figure 19 shows how the water level position was selected with the help of the fix red rulers. The ruler on the left indicates how the incident wave is evolving in time - since it is located in the lane of the swimmer - whereas the ruler on the right indicates how the transmitted wave is evolving in time - since it is located in the empty lane -.

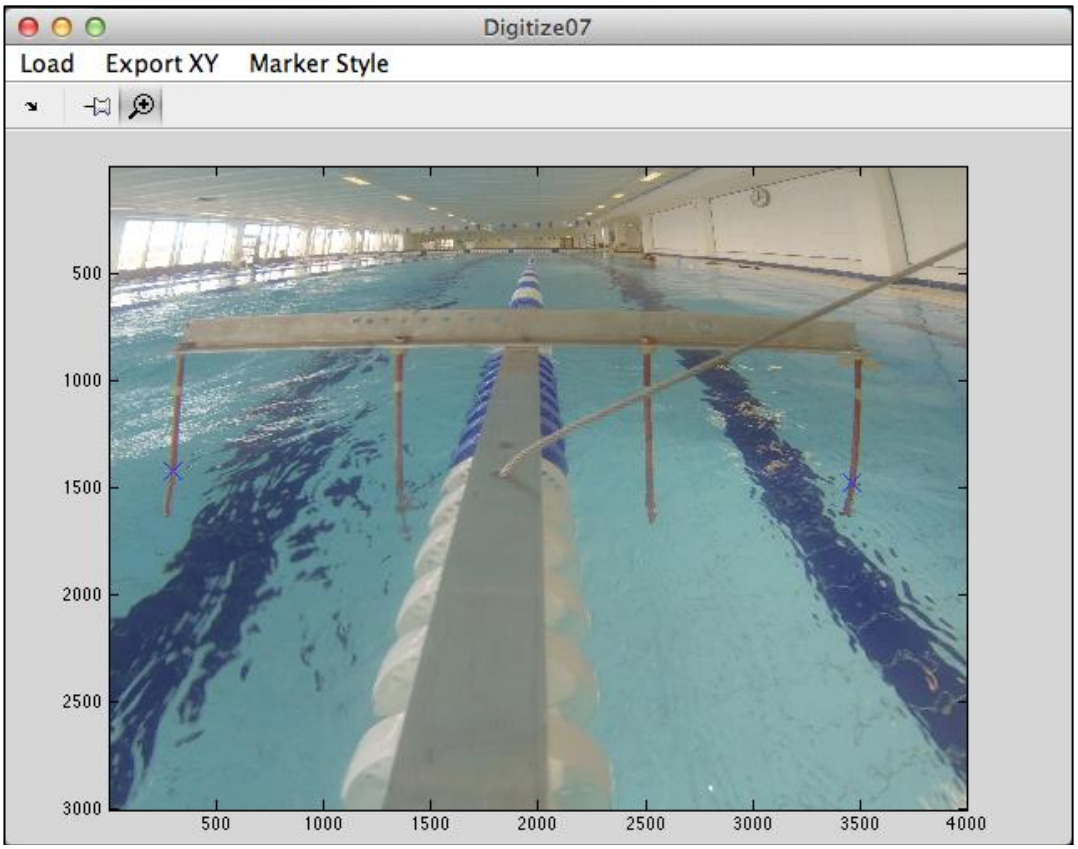

Figure 19: Example on how the wave height is manually selected for picture 20 of the series d5-br-ma-1.

4.4.3 Conversion into real coordinates

The coordinates for the water surface were defined on a plane that depended on the orientation of the camera. In order to get the real-world coordinates a transformation should be carried out based on the placement of the camera. Figure 20 provides a sketch of the experimental setup, where the camera is assumed to be oriented an angle β to the horizontal. In order to define the location of the water surface, the length z in Figure 20, that is, the distance from the top of the vertical bar to the water surface, is required. However, digitizing the image will yield the length z', which is z projected on the camera plane.

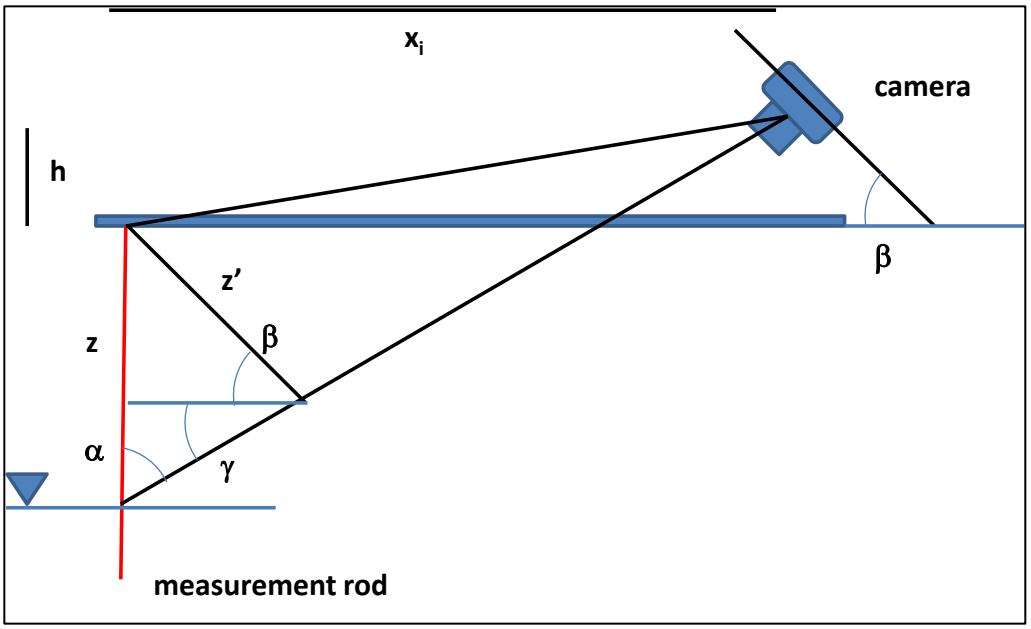

Figure 20: Sketch of measurement setup and definition of quantities needed to convert digitized lengths to real-world lengths.

From geometry a relationship may be derived between z and z'. It is assumed that x_i, h, and β are known and z' is given from the digitized image. The angle α is calculated from:

$$\tan\alpha = \frac{x_i}{h+z} \tag{10}$$

Using the law of sines:

$$\frac{\sin\alpha}{z'} = \frac{\sin(\beta+\gamma)}{z} \tag{11}$$

Furthermore, $\gamma = \pi/2-\alpha$ and introducing $\beta' = \beta + \pi/2$, the previous expression may be writen as:

$$z = z'\frac{\sin(\beta'-\alpha)}{\sin\alpha} \tag{12}$$

Expanding the numerator gives:

$$\sin(\beta'-\alpha) = \sin\beta'\cos\alpha - \cos\beta'\sin\alpha \tag{13}$$

Additional expansion yields:

$$\sin\beta' = \sin\left(\beta + \frac{\pi}{2}\right) = \cos\beta$$
$$\cos\beta' = \cos\left(\beta + \frac{\pi}{2}\right) = -\sin\beta \tag{14}$$

Substituting Eqs. 13 and 14 into Eq. 12 results in:

$$z = z'\left(\frac{\cos\beta}{\tan\alpha} + \sin\beta\right) \tag{15}$$

Replacing tan α in Eq. 15 using Eq. 10 gives after some rearrangement:

$$z = \frac{z'\left(\cos\beta\frac{h}{x_i} + \sin\beta\right)}{1 - \frac{z'}{x_i}\cos\beta} \tag{16}$$

Thus, using Eq. 16 the real length z may be derived from the digitized length z' and information about the camera placement. Knowing x_i, h, and β, the conversion factor is constant and the relationship between z and z' becomes a simple linear function. To this factor should another constant be added that relates distances obtained in the relative coordinate system used for the digitization to real-world distances. This constant was obtained through calibration against known distances from markings on the vertical bars.

4.5 Analysis

The real coordinates obtained after conversion were used to derive the evolution of the wave in time. Each series of 30 pictures taken during 3 seconds allowed for constructing plots similar to those in figure 21 and figure 22. The left bar located in the lane of the swimmer will give the evolution of the incident wave (red in the

figures), while the right rod located in the empty lane will give the evolution of the transmitted wave that has been damped (blue in the figures).

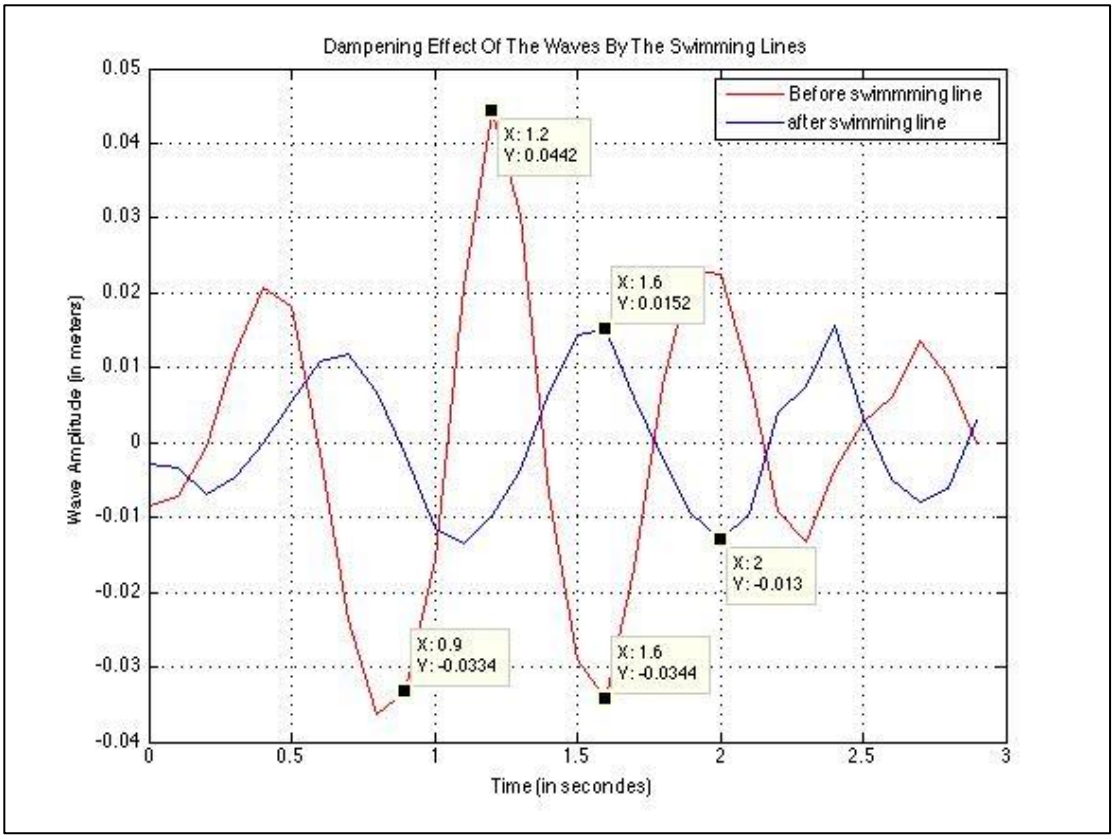

Figure 21: Incident and transmitted wave from experimental case d5-br-ma-1.

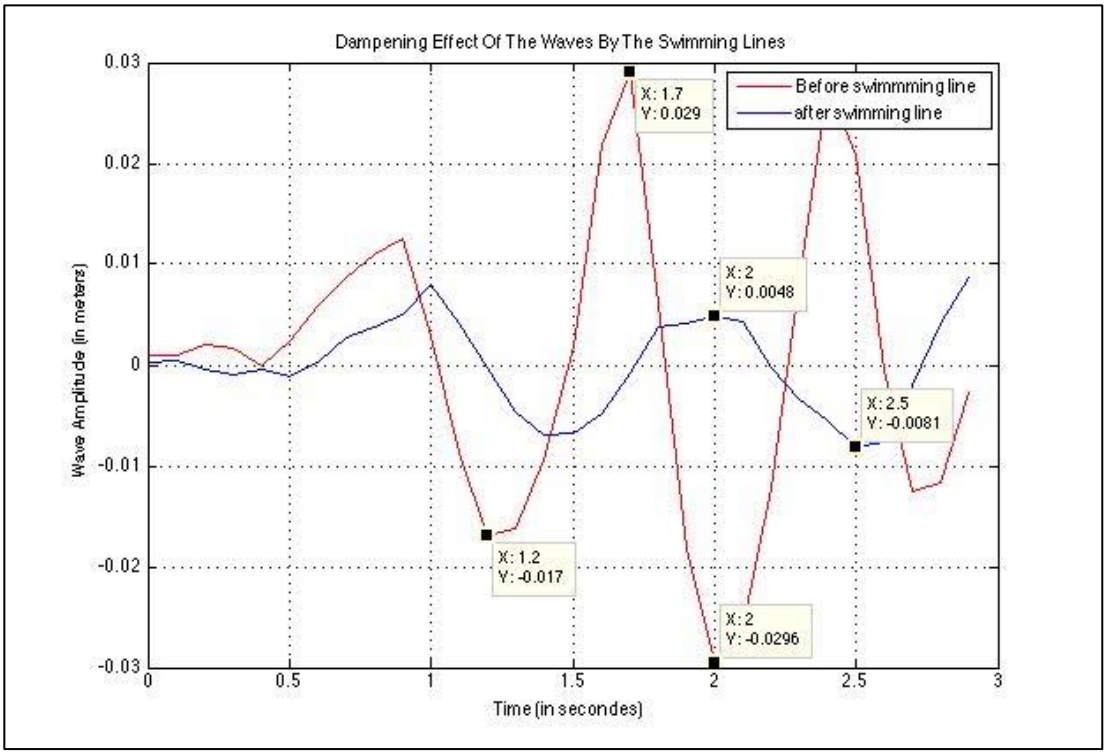

Figure 22: Incident and transmitted wave from experimental case d4-br-na-3.

Figures 21 and 22 show the coordinates of some characteristics points in the graphs, which make it possible to determine the incident wave height H_{in} and the transmitted wave height H_{out}. The characteristic coefficients defined previously can be obtained from (values given in table 2):

$\varepsilon_d = \frac{H_{out} - H_{in}}{Hin} = 1 - \varepsilon_t$: Damping coefficient

$\varepsilon_t = \frac{H_{out}}{Hin}$: Transmission coefficient

Series	H (cm)	M (Kg)	v (m/s)	Ti (s)	To (s)	Hi (cm)	Ho (cm)	ε_d (%)	ε_t (%)
d5-br-ma-1	168	63	1,15	0,7	0,6	7,86	2,82	64	36
d4-br-na-3	177	70	0,83	0,8	1,1	5,86	1,29	78	22

Table 2: Analysis of results from two experimental cases (data shown in figure 21 and figure 22).

Table 2 compares the efficiency of the swimming lines for the two experimental cases d4-br-na-3 and d5-br-ma-1. It can be deduced that the swimming lines were more efficient for the series from day 4 than for the series from day 5, since only about 22 % of the wave height was transmitted (78% of it was damped) for the former case.

One can arguably assume that the gold version of the swimming lines used in day 4 is simply more efficient in damping waves than the standard version used in day 5. However, it should be noted that these two series include different swimmers of different shapes, also swimming at different speeds. Apart from the type of line used, several other parameters will influence the damping efficiency. Those parameters are discussed in depth in section 5.

5 Data Analysis Results

In this section, the efficiency of swimming lines to dampen waves generated by swimmers will be analysed and discussed. Initially, some important general properties will be studied like the consistency of the period, the transmission coefficient, and the damping coefficient.

Furthermore, four important parameters will be analysed which are the speed of the swimmer, the diameter of the swimming line, the tension in the wire holding the line, and the swimming stroke employed. Indeed, the comparison between the competitor racing lane standard and the competitor racing lane gold, as well as the swimmer's speed and the different tension in the wire, will help to derive some general trends and principles concerning the behaviour of the lines. Consequently, those principles may be applied to improve the efficiency of the current racing lines manufactured by the company.

5.1 Period comparison

The wave period is one of the most important parameters, if not the most important one regarding the wave transmission. It was calculated before and after the waves impinge on the swimming line. The wave period was expected not to change since it is the same wave that is being analysed on both sides of the line. Figure 23 shows a clear linear relationship between the incident wave period Ti and the transmitted wave period To. The range of the period goes from 0.4s to 1s and the standard deviation is around 0.1s.

This period comparison was carried out for all the series analysed experimentally, which gives some credibility to the rest of the analysis demonstrating that the same waves were studied before and after damping. Finally, figure 23 shows only 23 points even though this comparison was made for all of the 93 time series. However, the explanation is that a large number of series have the same incident and transmitted wave period.

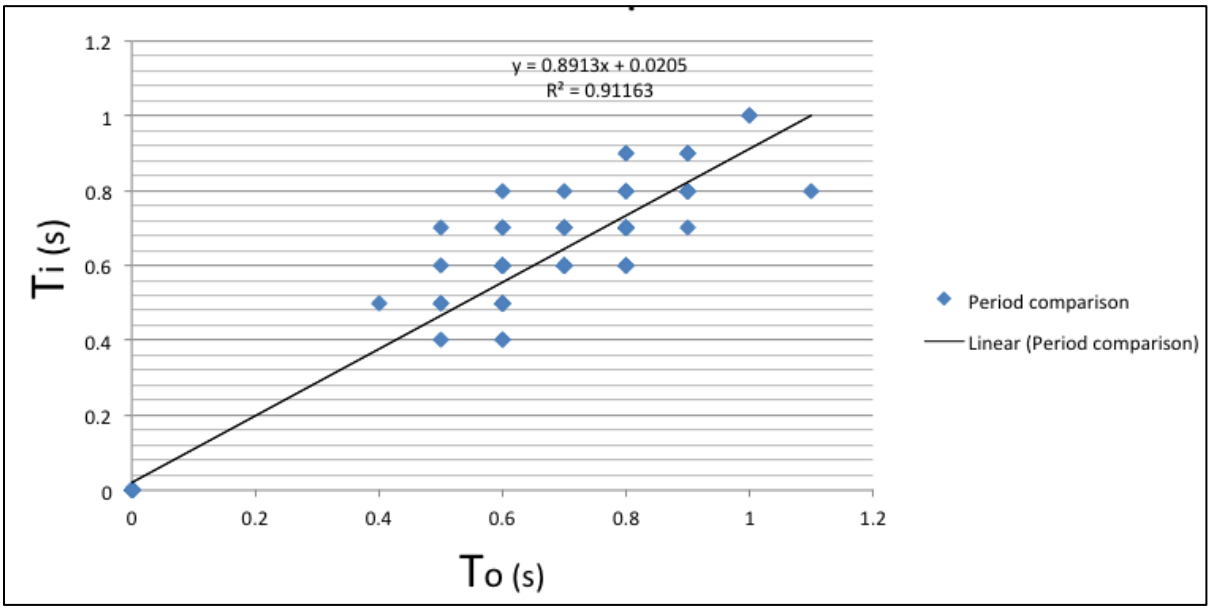

Figure 23: Relationship between incident and transmitted wave period.

5.2 Transmission coefficient

The transmission coefficient ε_t, as defined previously, is the ratio between the transmitted wave height and the incident wave height (employing the maximum wave height in the time series). It indicates the percentage of the wave that is being transmitted to the adjacent lane. The lower this coefficient is, the more efficient is the swimming line. This coefficient was calculated for all the series and was first studied without distinguishing between different swimmers, their speed, their stroke etc.

The results are shown in figure 24, which displays a scattered area of points that have, however, a certain structure or tendency. A linear fit was employed, which gives a first overall, estimate of ε_t that is approximately 32%, implying that 68%[4] of the waves is being damped.

[4] In reality this value should be slightly lower since it includes a part of the reflected wave. However, in the study the reflected part was assumed to be negligible compared to the transmitted one as confirmed by visual observations.

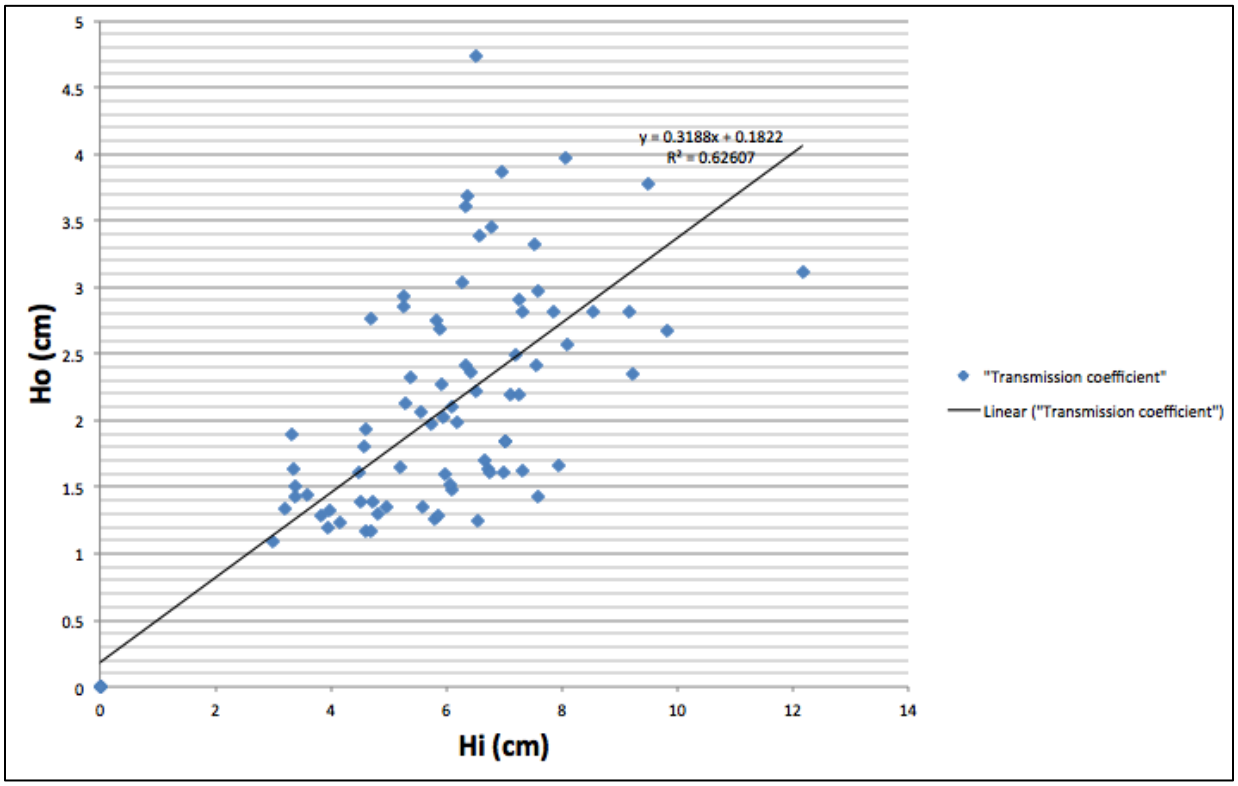

Figure 24: Incident and transmitted wave heights for all experimental cases studied.

5.3 Damping coefficient

The damping coefficient was deduced for the waves in each time series of pictures using the transmission coefficient calculated previously based on the image analysis. Swimming line manufacturers always try to produce swimming lines with a higher damping coefficient. It represents the percentage of the waves that is being absorbed or dissipated by the line.

Figure 25 displays a histogram that describes the distribution of the damping coefficient for the 93 different experimental cases studied. It shows that the median damping coefficient is approximately $\varepsilon_d \approx 70\%$, whereas the average of the 93 cases yields a mean value of $\varepsilon_d \approx 64\%$.

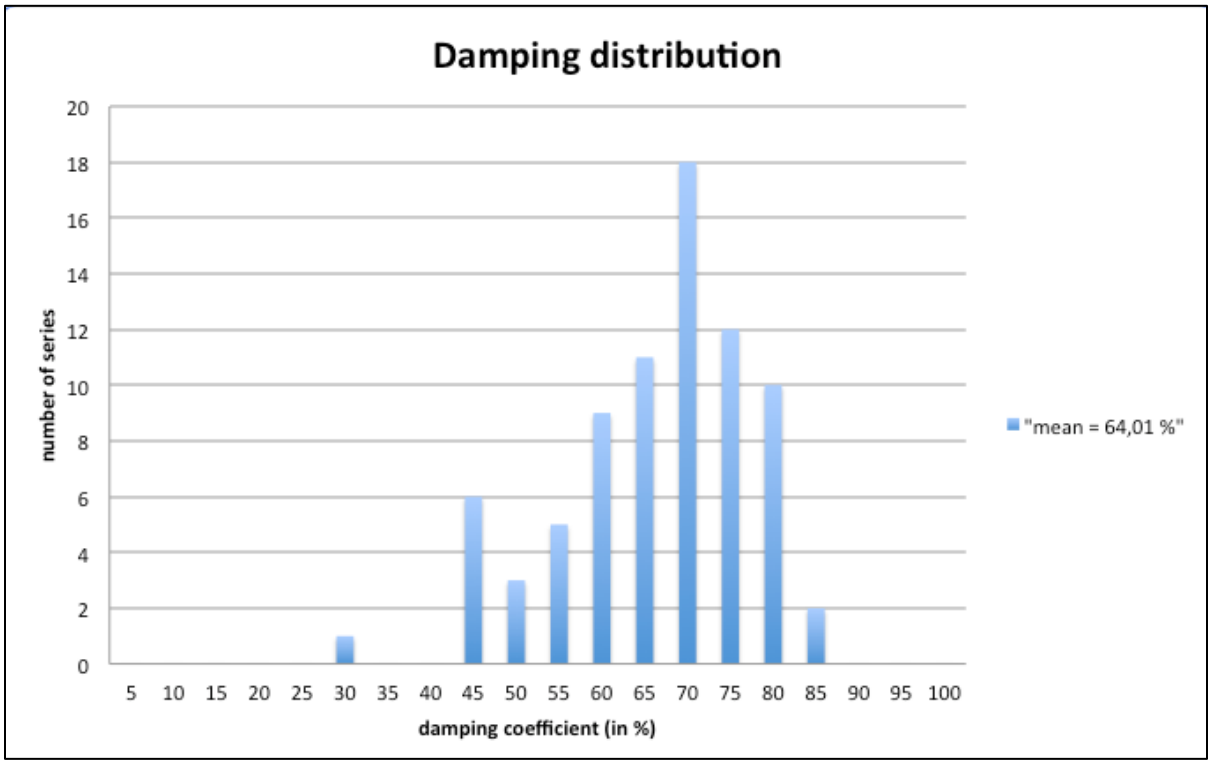

Figure 25: Histogram showing the distribution of the damping coefficient for the experimental cases studied

5.4 Speed effects of the swimmers

The speed of the swimmer is certainly one of the most interesting parameters to analyse. The transmission coefficients were calculated for the tests made during day 3, 4, and 5 by amateur swimmers and compared with the ones obtained during day 7 for the more professional swimmers.

The results are illustrated in figure 26 and shows that for day 3, 4, and 5 the transmission coefficient is $\varepsilon_t \approx 51\%$, whereas it is approximately 25% for day 7. Thus, the swimming lines are twice as efficient when the swimmers are swimming at higher speeds (1.5m/s on average for day 7) compared to when they are swimming at lower speeds (0.95m/s on average for day 3, 4, and 5).

In other words, figure 26 shows that the slope - which represents ε_t - is the same for day 3, 4, and 5 and, but it is much steeper than the slope obtained for day 7. Since the slope is the same for day 3, 4, and 5, it proves that despite using different lines

(day 5), the damping coefficient is still the same for low swimming speeds. Consequently, the speed could be considered as a predominant factor over the type of swimming lines.

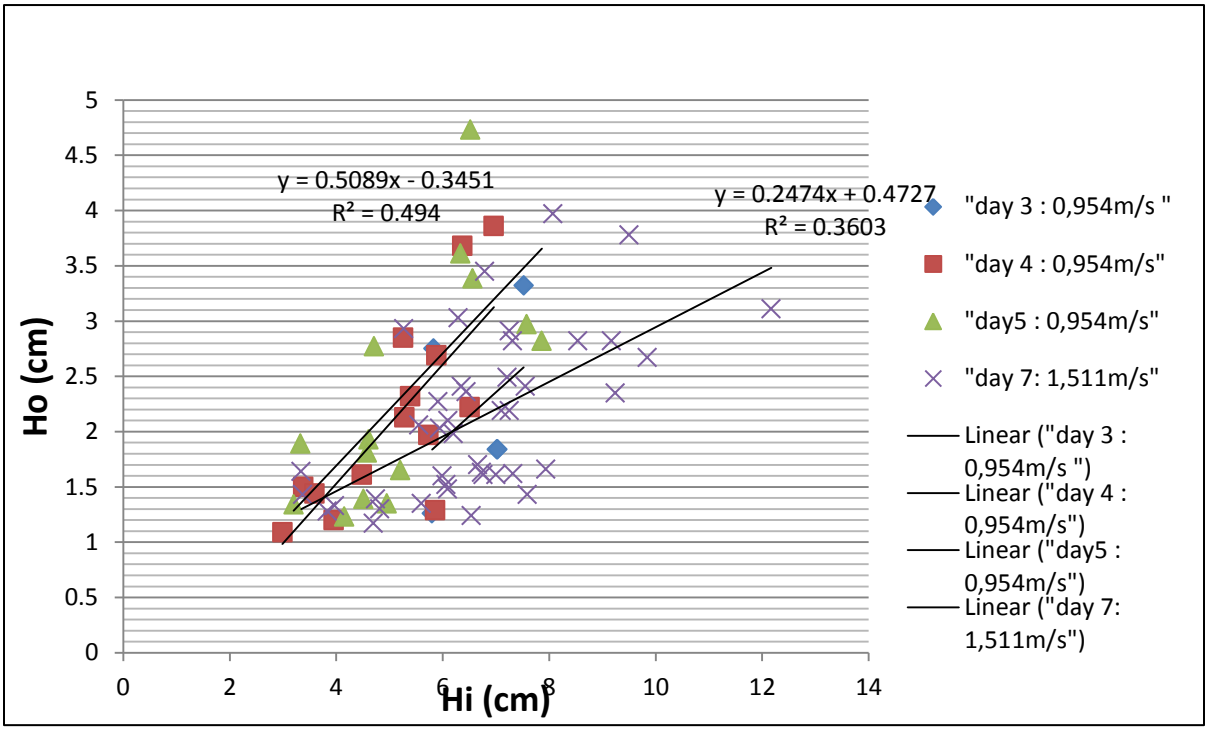

Figure 26: Transmitted wave height as a function of incident wave height for different speeds during days 3, 4, 5, and 7.

5.5 Comparison of different swimming lines

In this section, the efficiencies of the two different types of competitor racing lines were compared. The standard version of the lines that was used in the tests during day 5 is compared to the gold version used in the tests the other days.

Figure 27 illustrates the transmission coefficient for the standard line (data points in red), which is approximately $\varepsilon_t \approx 51\%$, whereas for the golden version of the lines (data points in blue) the coefficient is $\varepsilon_t \approx 25\%$.

The gold version of the swimming lines appears to be twice as efficient as the standard version, which can probably be explained by their diameter being

considerably larger (15cm compared to 10cm, respectively). There seems to be an almost linear relationship between the diameter of the swimming line and the transmission coefficient. Nevertheless, more detailed investigations should be made on a wider range of geometries to confirm these first results. Also, as pointed out in Section 5.4, there is an effect of the speed.

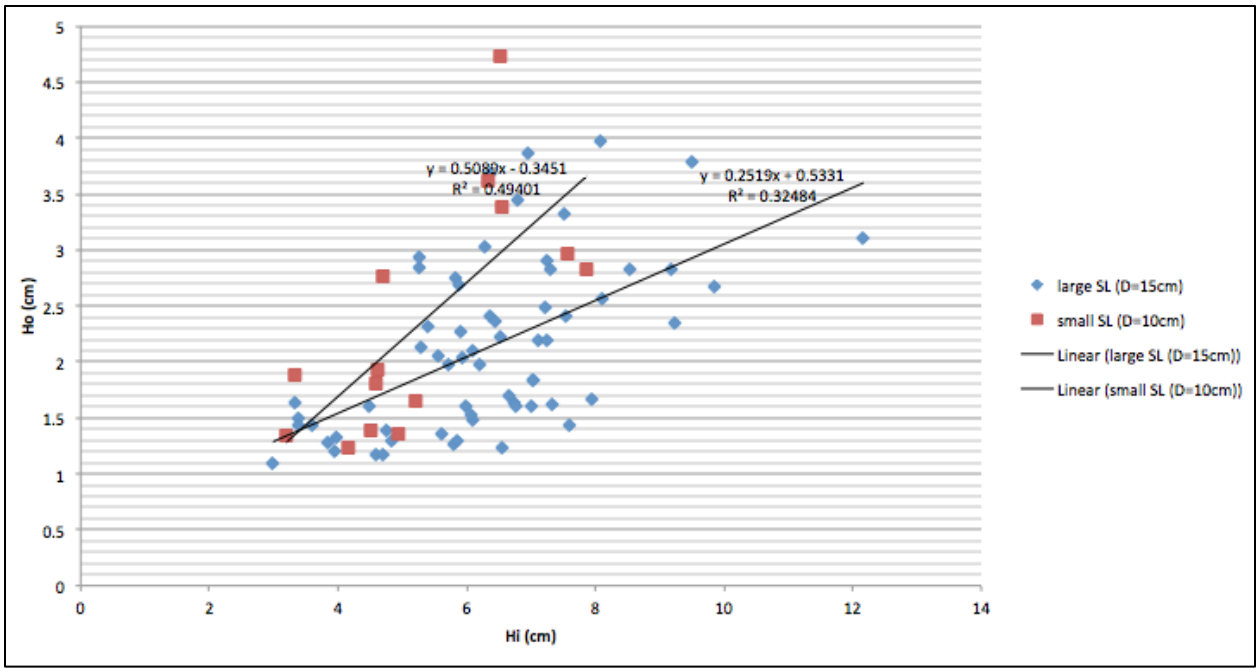

Figure 27: Transmitted wave height as a function of incident wave height for the two swimming lines tested, the standard version (10cm) and the gold version (15cm).

5.6 Effects of the tension in the wire

A parameter that is less intuitive but that could play a crucial role in the damping efficiency of the lines is the tension in the wire holding it. This parameter was tested during day 7 of the experiments using the same swimmers. Seven different swimmers were asked to swim employing four different strokes with a normal, 'soft' tension in the wire during the first two rounds of testing. Before doing a last round of tests, the tension was increased to its maximum - denoted as 'hard'- in order to see the effects on the damping from the lines.

The analysis of this parameter is mainly qualitative, since there was no equipment available to measure the tension in the swimming line. The results are shown in figure 28. It can be seen from this figure that when the tension is increased the

damping efficiency of the lines decreases considerably. Indeed, the transmission coefficient changes from $\varepsilon_t \approx 18\%$ for the 'soft' tension to $\varepsilon_t \approx 33\%$ for the 'hard' tension.

The explanation for this phenomenon is that when the tension is too high, the swimming lines lose their small horizontal displacement that is used to absorb a part of the wave energy. Indeed, it acts like one single stiff element, which reduces substantially the damping efficiency.

5.7 Influence of swimming stroke

In order to compare the different swimming strokes studied, that is, crawl, breast, backstroke, and butterfly, the focus was put on the speed and the maximum wave height for each type of stroke.

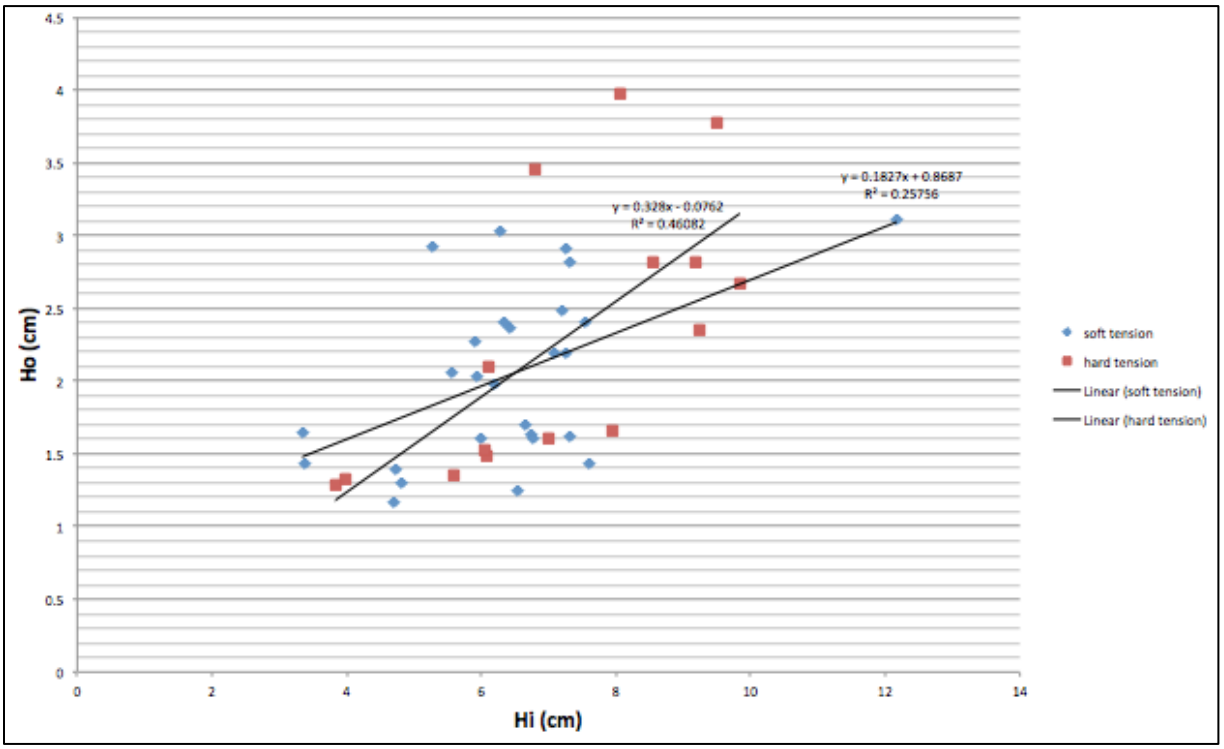

Figure 28: Transmitted wave height as a function of incident wave height for 'soft' and 'hard' tension in the line.

Figure 29 illustrates the relationship between the swimming speed and the maximum wave height generated for the four different strokes studied. It can be observed that when the swimmer's speed increases, the maximum wave height increases with it. However, what is surprising is that this growth is very similar four all kind of strokes, as indicated by the fact that the slopes of the lines in the figure 29 are more or less parallel.

Furthermore, it can be seen that the stroke that produces the highest waves is butterfly, followed by crawl, back stroke, and finally breast. It is understandable, since the butterfly stroke is the one that requires the most energy from the swimmer. Thus, there is a higher potential for the energy produced by the swimmer to be transformed it into surface waves.

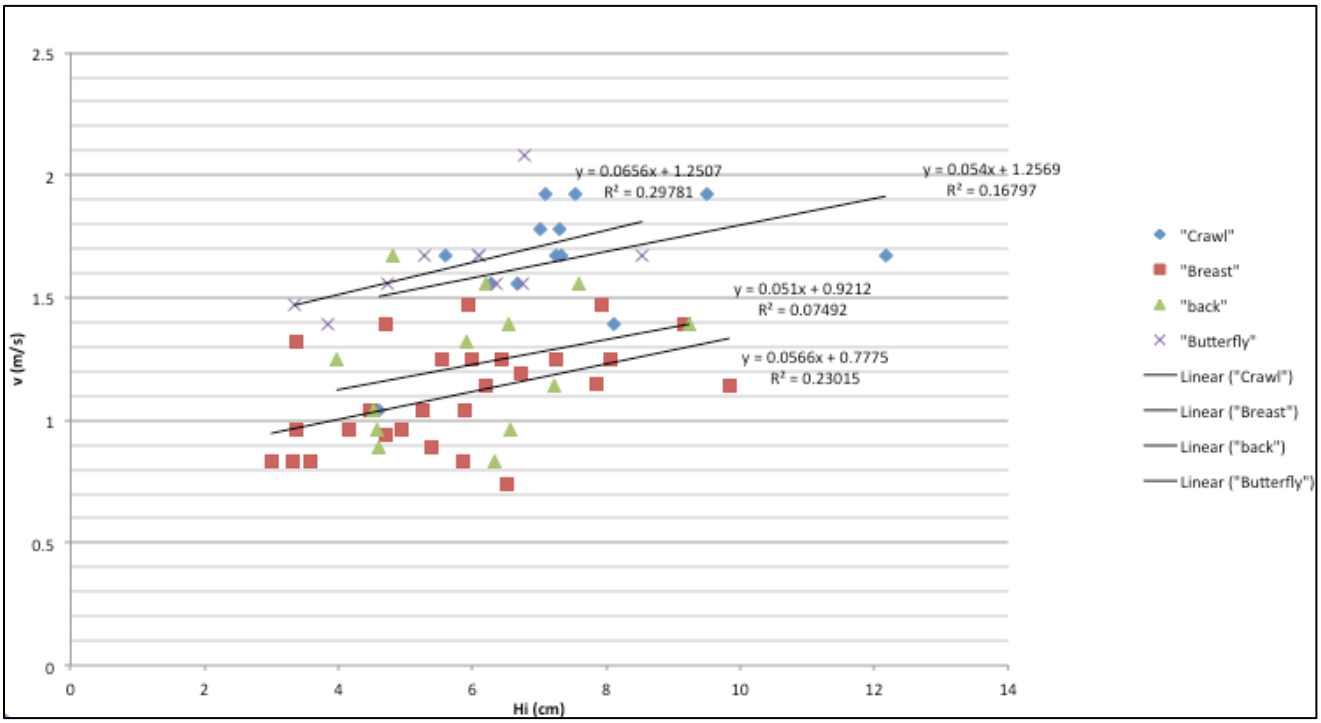

Figure 29: Relationship between swimming speed and generated maximum wave height for the four different swimming strokes investigated (crawl, breast, backstroke, and butterfly).

6 Conclusions

In summary, it was observed that the gold version of the swimming lines studied were twice as efficient in damping the waves generated by the swimmer compared to the standard version. It can partly be explained by the substantially larger diameter. A potential improvement for the current lines would be to manufacture a new type with a larger diameter, since the wave-damping efficiency seems to improve linearly with the size of the swimming lines. However, it is expected that there is an upper limit to this increase that should be investigated through additional studies.

Swimming lines were in general more efficient for professional swimmers rather than for amateurs. Indeed, the efficiency of the lines was considerably greater for high velocities associated with the professional swimmers. Consequently, for the crawl stroke, which in general is the fastest swimming style, the lines were very effective. The same remark could be made for the butterfly stroke, but for a different reason since it is the stroke that generates the highest waves. The swimming line was slightly less effective for back stroke and breast stroke.

The comparison of wave periods showed that the image procession method and the experimental tests done in general gave relevant results, even though the procedure itself was long and required meticulous work.

Indeed, one of the potential improvements of the measurement system could be to invest in capacitance or resistance gages, or laser technique, instead of using fixed vertical bars with rulers. This would avoid the tedious work of manually digitizing the water surface elevation. Such solutions have two major benefits: on one hand, it will save a considerable amount of time and therefore makes it possible to obtain more results in a shorter time; on the other hand the accuracy of the data collected will be greatly improved as well.

To sum up, more advanced tests, done on a wider scale would be necessary to confirm the first general principles observed in this investigation that has not been studied experimentally in detail before.

7 References

Online articles/journals:

Fairman, J. G, 1996. Buoyancy: Archimedes Principle. [online] National Aeronautics and space administration. Available at: http://www.grc.nasa.gov/WWW/k-12/WindTunnel/Activities/buoy_Archimedes.html [accessed 19 april 2013]

Kestin, J., Sokolov. M., Wakeham, W. A., 2004. *Viscosity of liquid water in the range -8˚C to 150˚C*. [online] Brown University, Providence, Rhode Islands 02912. Available at: http://www.nist.gov/data/PDFfiles/jpcrd121.pdf [accessed 2 may 2013]

Marinho, D. A., Rouboa, A. I., Alves, F. B., Villas-Boas, J.P., Machado, L., Reis, V. M., Silva, A.J., 2009. *Hydrodynamis analysis of different thumb positions in swimming* [online] Journal of Sports Science and Medicine. Available at: http://www.jssm.org/vol8/n1/9/v8n1-9pdf.pdf [accessed 30 april 2013]

Naemi, R., Easson, W. J., Sanders, R.H., 2010. *Hydrodynamic glide efficiency in swimming.* [online] Journal of Science and Medicine in sport 13. Available at: http://www.sciencedirect.com/science/article/pii/S1440244009001133 [accessed 9 january 2013]

Pallis, J.M., Mehta, R.D. 200?. *Aerodynamics and hydrodynamics in sports*. [online] available at: http://ebookbrowse.com/gdoc.php?id=321493265&url=60b6c1ee488e5f1bc07b93d69c8cf4ad [accessed 25 february 2013]

Toussaint, M. H., Hollander, A. P., Van den Berg, C., Vorontsov, A. 2000. *Biomechanics of swimming*. [online] available at: http://koreaswimming.co.kr/pds/Garrett-swimming.pdf [accessed 25 january 2013]

Vennell, R., Pease, D., Wilson, B. 2006. *Wave drag on human* swimmers. [online] Journal of Biomechanics 39. Available at: http://www.sciencedirect.com/science/article/pii/S0021929005000576 [accessed 14 january 2013]

Vilas-Boas, J.P., Silva ,D., Fernandes, R., Gonçalves, P., Figueiredo, P., Pereira, S., Roeseler, H., Machado, L. 2010. *Measuring the wave dissipation produced by swimming-line separation rope*. [online] International Symposium on Biomechanics

in Sports. Available at: http://connection.ebscohost.com/c/articles/59696275/measuring-wave-dissipation-produced-by-swimming-line-separation-rope [accessed 22 february 2013]

Vorontsov, A.R., Rumyantsev, V.A. 2008. *Biomechanics in Sport: Performance Enhancement and Injury Prevention.* [online] Blackwell Science Ltd, Oxford, UK. Available at: http://onlinelibrary.wiley.com/doi/10.1002/9780470693797.ch9/summary [accessed 14 fevruary 2013]

Websites:

CEM -Coastal Engineering Manual-, 2008, CEM wave. [online] Available at: http://chl.erdc.usace.army.mil/chl.aspx?p=s&a=ARTICLES;101 [Accessed 28 may 2013]

FINA World Championship Classroom Resource, 2007. Swimming it's a Drag. [online] Available at: http://www.publish.csiro.au/video/projects/FINA/sections/teach/swimming_itsadrag.html [Accessed 20 April 2013]

GoPro HERO 3 Black Edition, 2013. Features. [online] Available at: http://gopro.com/cameras/hd-hero3-black-edition#features [Accessed 28 april 2013]

Hill, K., 2012. Food coloring, fluid dynamics, and an awesome lab demo. [online] Available at: http://www.lukor.net/2012/10/17/food-coloring-fluid-dynamics-and-an-awesome-lab-demo/ [Accessed 14 may 2013]

Malmsten company, 2013. Competitor-Racing lanes. [online] Available at: http://www.malmsten.com/main/default.asp?catid=23&sid=78&subcatid=78&langid=2&id=9&menu=1 [Accessed 4 march 2013]

Riyeka, K. Technical F1 Dictionnary, 2011. [online] Available at: http://www.formula1-dictionary.net [Accessed 17 may 2013]

Books:

Clarys, J. P., 1978. *Relationship of human body form to passive and active hydrodynamic drag.* In Biomechanics VI-B (eds E. Asmussen & K. Jorgensen). Uniersity Park Press. Baltimore

Schleihauf, R.E., 1979. A Hydrodynamic Analysis of Swimming Propulsion, Swimming III. International Series of Sports Sciences, Vol. 8. University Park Press, Baltimore, MD, pp. 70–117.

Lecture notes:

Larson, M., 2013. Pressure and Friction Drag I, VVR90 Hydromechanics, Lund University, unpublished.

8 List of figures and tables

9 Appendices

9.1 Cases investigated

The lines in blue refer to the series that have some data missing. Sometimes it was difficult to extract water level information, which in turn implied uncertainties regarding the wave period and the wave height.

Series	Stroke	Name	Height (cm)	Weight (Kg)	V (m/s)	Ti (s)	To (s)	Hin (cm)	Hout (cm)
d3-cr-ra-1	Crawl	Raphaello	180	75	0,83	0,6	0,8	7,02	1,84
d3-cr-ra-1'	Crawl	Raphaello	180	75	0,83	0,6	0,8	7,03	1,84
d3-cr-ra-2	Crawl	Raphaello	180	75	0,89	0,6	0,7	5,83	2,75
d3-cr-ra-3	Crawl	Raphaello	180	75	0,78	0,5	0,6	5,8	1,26
d3-cr-ra-4	Crawl	Raphaello	180	75	0,89	1	1	7,52	3,32
d4-br-em-3	Breast	Emma	165	57	0,96	0,5	0,4	3,38	1,5
d4-br-em-4	Breast	Emma	165	57	0,83	0,6	0,6	3,59	1,44
d4-br-em-5	Breast	Emma	165	57	0,83	0,4	0,6	2,99	1,09
d4-cr-jo-1	Crawl	Joel	191	85	0,96	0,6	0,6	5,28	2,13
d4-cr-jo-3	Crawl	Joel	191	85	1,04	0,6	0,6	6,96	3,86
d4-cr-jo-5	Crawl	Joel	191	85	1,04	0,6	0,6	6,37	3,68
d4-br-jo-2	Breast	Joel	191	85	1,04				
d4-br-jo-3	Breast	Joel	191	85	1,04	0,5	0,6	5,26	2,85
d4-br-jo-4	Breast	Joel	191	85	1,04	0,5	0,6	5,88	2,69
d4-cr-na-1	Crawl	Nadim	177	70	1,39	0,6	0,7	6,51	2,22
d4-cr-na-2	Crawl	Nadim	177	70			0	3,95	1,2
d4-cr-na-3	Crawl	Nadim	177	70	1,39	0,7	0,8	5,73	1,97
d4-br-na-1	Breast	Nadim	177	70	1,04	0,7	0,8	4,48	1,61
d4-br-na-2	Breast	Nadim	177	70	0,89	0,7	0,7	5,39	2,32
d4-br-na-3	Breast	Nadim	177	70	0,83	0,8	1,1	5,86	1,29
d5-cr-ma-1	Crawl	Maike	168	63	1,25	0,4	0,5	5,2	1,65

d5-cr-ma-2	Crawl	Maike	168	63	1,25				
d5-br-ma-1	Breast	Maike	168	63	1,15	0,7	0,6	7,86	2,82
d5-br-ma-2	Breast	Maike	168	63	0,94	0,6	0,7	4,71	2,77
d5-br-ma-3	Breast	Maike	168	63	0,74	0,7	0,8	6,52	4,73
d5-ba-ma-1	Back	Maike	168	63	0,89	0,6	0,5	4,61	1,93
d5-ba-ma-2	Back	Maike	168	63	0,96	0,6	0,6	4,58	1,81
d5-ba-ma-3	Back	Maike	168	63	1,04	0,4	0,6	4,51	1,39
d5-cr-mar-1	Crawl	Marten	185	88	1,04	0,7	0,6	3,2	1,34
d5-cr-mar-2	Crawl	Marten	185	88	0,96	0,8	0,9	7,58	2,97
d5-cr-mar-3	Crawl	Marten	185	88	0,96				
d5-br-mar-1	Breast	Marten	185	88	0,96	0,7	0,7	4,15	1,23
d5-br-mar-2	Breast	Marten	185	88	0,96	0,8	0,6	4,95	1,35
d5-br-mar-3	Breast	Marten	185	88	0,83	0,6	0,8	3,33	1,89
d5-ba-mar-1	Back	Marten	185	88	0,96	0,7	0,7	6,56	3,385
d5-ba-mar-2	Back	Marten	185	88	0,83	0,7	0,8	6,33	3,61
d6-cr-mic-1	Crawl	Michael	175	72	1,39	0,7	0,7	8,11	2,57
d6-cr-mic-2	Crawl	Michael	175	72	1,04	0,6	0,6	4,6	1,17
d7-cr-pa-1	Crawl	Pablo	185	78	1,92	0,8	0,8	7,55	2,41
d7-cr-pa-2	Crawl	Pablo	185	78	1,78	0,6	0,8	7,31	2,82
d7-cr-pa-3	Crawl	Pablo	185	78	1,92	0,8	0,8	9,5	3,78
d7-br-pa-1	Breast	Pablo	185	78	1,25	0,6	0,7	7,25	2,91
d7-br-pa-3	Breast	Pablo	185	78	1,47	0,7	0,8	7,94	1,66
d7-ba-pa-1	Back	Pablo	185	78	1,67	0,8	0,7	4,82	1,3
d7-bu-pa-2	Butterfly	Pablo	185	78	1,56	0	0	0	0
d7-bu-pa-3	Butterfly	Pablo	185	78	2,08	0,8	0,8	6,79	3,45
d7-cr-gu-1	Crawl	Gustav	182	63	1,56	0,6	0,7	6,29	3,03
d7-br-gu-1	Breast	Gustav	182	63	1,25	0,5	0,5	5,55	2,06
d7-br-gu-2	Breast	Gustav	182	63	1,39	0,6	0,6	4,7	1,17
d7-br-gu3	Breast	Gustav	182	63	1,32	0	0	0	0
d7-ba-gu-1	Back	Gustav	182	63	1,56	0,5	0,6	7,59	1,43
d7-ba-gu-3	Back	Gustav	182	63	1,39	0	0	9,24	2,35

d7-bu-gu-1	Butterfly	Gustav	182	63	1,67	0	0	5,27	2,93
d7-bu-gu-3	Butterfly	Gustav	182	63	1,67	0,6	0,8	6,1	2,1
d7-cr-ag-2	Crawl	Agnes	175	70	1,67	0,8	0,9	12,17	3,11
d7-cr-ag-3	Crawl	Agnes	175	70	1,78	0,7	0,8	7	1,61
d7-br-ag-1	Breast	Agnes	175	70	1,47	0,6	0,7	5,94	2,03
d7-br-ag-3	Breast	Agnes	175	70	1,39	0,7	0,8	9,17	2,82
d7-ba-ag-3	Back	Agnes	175	70	1,39	0	0	0	0
d7-bu-ag-2	Butterfly		175	70	1,47	0,7	0,5	3,34	1,64
d7-cr-pe-1	Crawl	Peter	179	68	1,92	0,8	0,9	7,1	2,19
d7-cr-pe-2	Crawl	Peter	179	68	1,67	1	1	7,25	2,19
d7-br-pe-1	Breast	Peter	179	68	1,32	0,9	0,8	3,37	1,43
d7-br-pe-3	Breast	Peter	179	68	1,39	0	0	0	0
d7-ba-pe-2	Back	Peter	179	68	1,14	0,8	0,9	7,21	2,49
d7-ba-pe-3	Back	Peter	179	68	1,25	0,5	0,6	3,97	1,33
d7-bu-pe-2	Butterfly	Peter	179	68	1,56	0,5	0,5	6,35	2,41
d7-bu-pe-3	Butterfly	Peter	179	68	1,67	0,6	0,6	6,09	1,48
d7-cr-si-2	Crawl	Simon	182	77	1,67	0,7	0,8	7,32	1,62
d7-cr-si-3	Crawl	Simon	182	77	1,67	0,5	0,6	5,6	1,35
d7-br-si-1	Breast	Simon	182	77	1,25	0,7	0,8	5,99	1,6
d7-br-si-3	Breast	Simon	182	77	1,14	0,6	0,7	9,84	2,67
d7-ba-si-1	Back	Simon	182	77	1,56	0,6	0,6	6,2	1,98
d7-ba-si-3	Back	Simon	182	77	1,47	0	0	0	0
d7-cr-jos-1	Crawl	Josephina	169	58	1,67	0	0	0	0
d7-br-jos-1	Breast	Josephina	169	58	1,14	0,9	0,8	6,73	1,63
d7-br-jos-2	Breast	Josephina	169	58	1,19	0,7	0,9	6,44	2,36
d7-br-jos-3	Breast	Josephina	169	58	1,25	0,8	0,9	8,07	3,97
d7-ba-jos-1	Back	Josephina	169	58	1,32	0,5	0,6	5,91	2,27
d7-ba-jos-2	Back	Josephina	169	58	1,39	0	0	6,54	1,24
d7-ba-jos-3	Back	Josephina	169	58	1,67	0	0	0	0
d7-bu-jos-1	Butterfly	Josephina	169	58	1,56	0,6	0,6	6,76	1,61
d7-bu-jos-2	Butterfly	Josephina	169	58	1,56	0	0	0	0

d7-bu-jos-3	Butterfly	Josephina	169	58	1,39	0,9	0,9	3,83	1,28
d7-cr-be-2	Crawl	Bella	171	72	1,56	0,6	0,7	6,66	1,7
d7-cr-be-3	Crawl	Bella	171	72	1,31	0	0	0	0
d7-br-be-1	Breast	Bella	171	72	1,39	0	0	0	0
d7-br-be-2	Breast	Bella	171	72	1,25	0	0	0	0
d7-br-be-3	Breast	Bella	171	72	1,25	0,9	0,9	6,06	1,52
d7-ba-be-1	Back	Bella	171	72	1,32	0	0	0	0
d7-bu-be-1	Butterfly	Bella	171	72	1,56	0,9	0,9	4,74	1,39
d7-bu-be-3	Butterfly	Bella	171	72	1,67	0,8	0,9	8,54	2,82

Table 3: Complete table showing the basic results extracted from the 93 series of pictures taken from day 3 to day 7.

9.2 Wave height selection

The Matlab routine called “digitize07.m” which made the water level digitization and subsequent wave height selection possible:

```
function digitize07(varargin)
%DIGITIZE07  Digitze points on an image using the mouse
%   DIGITIZE07(filename) displays an image and allows the
user to
%   digitize points using the mouse, similar to MATLAB's
built-in GINPUT
%   and similar to other digitizers available at the MATLAB
Central File
%   Exchange: 'digitize','digitize2.m', etc.  The main new
feature of
%   this version is that points are draggable; this permits
fine tuning
%   of already digitized points using the zoom feature.
%
%   Other features adopted from previous versions include:
%       - Import previously digitized points
%       - Export digitized points to the workspace or file
%       - Interactively change the marker color, size, and
shape
%       - Pin digitized points (i.e. toggle draggable mode)
%       - Delete unwanted points by right-clicking on the
point
%       - Fully interactive GUI:  Errors are reported to
dialog boxes
%         rather than to the Workspace
%
%   DIGITIZE07(filename) opens an interactive GUI and allows
the user to
%   digitize an unlimited number of points.  The file must be
an image that
%   is recognized by IMREAD
%
%   DIGITIZE07 by itself opens the digitizer and prompts the
use to load an image file
%
%
%USING THE GUI:
% (a) Digitizing points.  Point-and-click (left or right
button to create a new point).
% (b) Drag a new point.  Hold the button you used to create
```

```
the point and
%     drag it to a new location.  A point may be dragged
anywhere within
%     the axes boundaries.
% (c) Drag an existing point.  Left-click and hold to drag.
% (d) Disable/enable drag.  Use the pin toggle button on the
left of the
%     figure's toolbar.  This will pin all existing points.
New points are
%     still draggable.
% (e) Other features.  Other menu features and the zoom tool
are self-explanatory.
%
%
%   See also GINPUT
%
%
%   Acknowledgements:
%   This was developed based on the functions "draggable" and
"digitize2"
%   which are both available from the MATLAB Central File
Exchange.
%
%   Author:
%   Todd C Pataky (0todd0@gmail.com)  ['zero' todd
'zero'@gmail.com]
%   18-April-2007


%IMPLEMENTATION NOTES:
%   1. The handles of digitized points are stored as
application data in
%   the image's axes.  These handles are passed into
different callback
%   functions which allows for easy implementation of
dragging using the
%   figure properties: WindowButtonMotionFcn and
WindowButtonUpFcn
%   2. The digitizer uses Figure 1 to open the image.  If
Figure 1 already
%   existis it will be cleared.
%   3. Features for a future version:
%       - Display point labels
%       - Reorder points
%       - Connect points
```

```
%       - Create reference axes
%       - Calibration (scale image coordinates to mm, m,
etc.)
%
```

```
%% PRELIMINARY DATA CHECKS

%%%%%%%%%%%%%%%%%%%%
%(1) Ensure proper argument specification:
%%%%%%%%%%%%%%%%%%%%
switch nargin
    case 0
        initializeFigure  %see INITIALIZATION FUNCTIONS below
        initializeAxes([])
    case 1
        try  %Attempt to initiate the GUI:
            imfinfo(varargin{1});  %This will generate an
error if not recognized by IMREAD
            initializeFigure
            initializeAxes(varargin{1})
        catch
            fprintf('\n\n\nError opening file.\n')
            fprintf('  Please ensure that the file exists\n')
            fprintf('  and that its format is recognized by
''imread.m''\n');
            error(lasterror)
        end
    otherwise
        error('Maximum of one input argument.')
end
%%%%%%%%%%%%%%%%%%%%
%(2) Check Workspace for existence of 'XY':
%%%%%%%%%%%%%%%%%%%%
if evalin('base','exist(''XY'');')==1
    msgbox(['The variable XY exists in the Workspace.
',...
        'Selecting ''Export XY''...''To Workspace'' will
overwrite the current XY data.'],...
        'Warning!','warn')
end
```

```
%% INITIALIZATION FUNCTIONS

function initializeFigure
figure(1)
clf
set(gcf,'numberTitle','off','name','Digitize07')
set(gcf,'menubar','none','closeRequestFcn',@closeFigure)
%%%%%%%%%%%%%%%%%%%%%%%%%
%CREATE MENU
%%%%%%%%%%%%%%%%%%%%%%%%%
%(a) Load functions
%%%%%%%%%%%%%%%%%%%%%%%%%
mh = uimenu(gcf,'Label','Load','separator','on');
uimenu(mh,'Label','Image...','callback',@callback_loadImage);
uimenu(mh,'Label','Points...','callback',@callback_loadPoints
);
%%%%%%%%%%%%%%%%%%%%%%%%%
%(b) Export functions
%%%%%%%%%%%%%%%%%%%%%%%%%
mh = uimenu(gcf,'Label','Export XY');
uimenu(mh,'label','To
Workspace','callback',@callback_export2Base)
uimenu(mh,'label','To .mat
File...','callback',{@callback_export2File,'.mat'},'separator
','on')
uimenu(mh,'label','To .dat
File...','callback',{@callback_export2File,'.dat'})
%%%%%%%%%%%%%%%%%%%%%%%%%
%(c) Marker style functions
%%%%%%%%%%%%%%%%%%%%%%%%%
mh = uimenu(gcf,'Label','Marker Style');
mh1 = uimenu(mh,'Label','Color');
    uimenu(mh1,'Label','Static
Color...','callback',@callback_changeStaticColor);
    uimenu(mh1,'Label','Dragging
Color...','callback',@callback_changeDragColor);
uimenu(mh,'Label','Size...','callback',@callback_changeMarker
Size);
```

```
mh2 = uimenu(mh,'Label','Symbol');
    uimenu(mh2,'Label','+  Plus
sign','callback',{@callback_changeSymbol,'+'})
    uimenu(mh2,'Label','o
Circle','callback',{@callback_changeSymbol,'o'})
    uimenu(mh2,'Label','*
Asterisk','callback',{@callback_changeSymbol,'*'})
    uimenu(mh2,'Label','.
Point','callback',{@callback_changeSymbol,'.'})
    uimenu(mh2,'Label','x
Cross','callback',{@callback_changeSymbol,'x'})
    uimenu(mh2,'Label','s
Square','callback',{@callback_changeSymbol,'s'})
    uimenu(mh2,'Label','d
Diamond','callback',{@callback_changeSymbol,'d'})
    uimenu(mh2,'Label','^  Triangle
(up)','callback',{@callback_changeSymbol,'^'},'separator','on
')
    uimenu(mh2,'Label','v  Triangle
(down)','callback',{@callback_changeSymbol,'v'})
    uimenu(mh2,'Label','>  Triangle
(right)','callback',{@callback_changeSymbol,'>'})
    uimenu(mh2,'Label','<  Triangle
(left)','callback',{@callback_changeSymbol,'<'})
    uimenu(mh2,'Label','p
Pentagram','callback',{@callback_changeSymbol,'p'},'separator
','on')
    uimenu(mh2,'Label','h
Hexagram','callback',{@callback_changeSymbol,'h'})
%%%%%%%%%%%%%%%%%%%%%%%%%
%CREATE TOGGLE ICONS:
%%%%%%%%%%%%%%%%%%%%%%%%%
ht = uitoolbar;
%%%%%%%%%%%%%%%%%%%%%%%%%
%(a) Pin points
%%%%%%%%%%%%%%%%%%%%%%%%%
[x,map] =
imread([matlabroot,'/toolbox/matlab/icons/pin_icon.gif']);
cdata = ind2rgb(x,map);
cdata(cdata==1)=NaN;
uitoggletool(ht,'cdata',cdata,'TooltipString','Pin
Points',...
    'onCallback', 'setappdata(gca,''pinPoints'',1)',...
    'offCallback','setappdata(gca,''pinPoints'',0)');
%%%%%%%%%%%%%%%%%%%%%%%%%
```

```
%(b) Zoom tool
%%%%%%%%%%%%%%%%%%%%%%%%%
fname = [matlabroot,'/toolbox/matlab/icons/zoomplus.mat'];
load(fname)  %var name: 'cdata' (stored in zoomplus.mat)
uitoggletool(ht,'cdata',cdata,'TooltipString','Zoom','clicked
Callback','zoom')




function initializeAxes(fname,varargin)
axes('position',[0.05 0.05 0.9 0.9])
%%%%%%%%%%%%%%%%%%%%%%%%%
%Initialize application data:
%%%%%%%%%%%%%%%%%%%%%%%%%
setappdata(gca,'axlim',[])  %required for dragging points
setappdata(gca,'H',[])
setappdata(gca,'pinPoints',0)
if nargin==1
    markerSpecs = struct('statColor',[0 0 1],'dragColor',[1 0
0],'size',6,'style','o');
    setappdata(gca,'markerSpecs',markerSpecs)
else setappdata(gca,'markerSpecs',varargin{1})
end

%%%%%%%%%%%%%%%%%%%%%%%%%
%Create message or display image
%%%%%%%%%%%%%%%%%%%%%%%%%
if isempty(fname)
    th = text(0.5,0.5,'Please load an image to begin.');

set(th,'fontsize',14,'horizontalalignment','center','vertical
alignment','middle',...
        'backgroundcolor',0.9*[1 1 1],'edgecolor','k')
    axis off
else displayImage(fname)
end




function displayImage(fname)
```

```
X = imread(fname);
ih = imagesc(X);
set(ih,'buttonDownFcn',@d07_createPoint)
axis equal tight
hold on
axlim = [get(gca,'xlim') get(gca,'ylim')];
setappdata(gca,'axlim',axlim)




%% MAIN DIGITIZING CODE

function d07_createPoint(varargin)
%%%%%%%%%%%%%%%%%%%%%%%%%
xy = get(gca,'CurrentPoint');  %CurrentPoint yields two
output rows
xy = xy(1,1:2);
h = d07_plotPoints(xy);
setappdata(gca,'H',[getappdata(gca,'H'); h])
%Enable dragging until button is released:
set(gcf,'WindowButtonMotionFcn',{@d07_dragPoint,h},'WindowBut
tonUpFcn',{@d07_buttonUp,h})




function [H] = d07_plotPoints(XY)
%%%%%%%%%%%%%%%%%%%%%%%%%
H = zeros(size(XY,1),1);
for k=1:size(XY,1)
    H(k) = plot(XY(k,1),XY(k,2),'.');
    %Create context menu for deleting points:
    cmenu = uicontextmenu;
    uimenu(cmenu, 'Label', 'Delete this point','Callback',
{@deletePoint,H(k)});
    uimenu(cmenu, 'Label', 'Delete all points...','Callback',
@deleteAllPoints,'separator','on');
    set(H(k),'UIContextMenu', cmenu)
end
markerSpecs = getappdata(gca,'markerSpecs');
set(H,'Color',markerSpecs.statColor,...
    'MarkerSize',markerSpecs.size,...
```

```
    'Marker',markerSpecs.style,...
    'ButtonDownFcn',@d07_clickPoint);




function d07_clickPoint(h,varargin)
%%%%%%%%%%%%%%%%%%%%%%%%%
if ~getappdata(gca,'pinPoints')
    markerSpecs = getappdata(gca,'markerSpecs');
    set(h,'color',markerSpecs.dragColor)

set(gcf,'WindowButtonMotionFcn',{@d07_dragPoint,h},'WindowBut
tonUpFcn',{@d07_buttonUp,h})
end




function d07_dragPoint(varargin)
%%%%%%%%%%%%%%%%%%%%%%%%%
h = varargin{3};
markerSpecs = getappdata(gca,'markerSpecs');
set(h,'color',markerSpecs.dragColor)
%%%%%%%%%%%%%%%%%%%%%%%%%
% Ensure that the dragged point lies within the axis bounds:
%%%%%%%%%%%%%%%%%%%%%%%%%
axlim = getappdata(gca,'axlim');
X = get(gca,'currentpoint');
[x,y] = deal(X(1,1),X(1,2));
if x<axlim(1)
    x=axlim(1);
elseif x>axlim(2)
    x=axlim(2);
end
if y<axlim(3)
    y=axlim(3);
elseif y>axlim(4)
    y=axlim(4);
end
%%%%%%%%%%%%%%%%%%%%%%%%%
% Update marker position
```

```
%%%%%%%%%%%%%%%%%%%%%%%%%
set(h,'xdata',x,'ydata',y)




function d07_buttonUp(varargin)
%%%%%%%%%%%%%%%%%%%%%%%%%
h = varargin{3};
markerSpecs = getappdata(gca,'markerSpecs');
set(h,'color',markerSpecs.statColor)
set(gcf,'WindowButtonMotionFcn',[],'WindowButtonUpFcn',[])




%% CALLBACK FUNCTIONS

function callback_loadImage(varargin)
%%%%%%%%%%%%%%%%%%%%%%%%%
% Check if there are existing points
if ~isempty(getappdata(gca,'H'))
    button = questdlg(['Loading a new image will clear
current points.  ',...
        'OK to continue?'],'Warning!!','OK','Cancel','OK');
    if isequal(button,'Cancel')
        return
    end
end
%%%%%%%%%%%%%%%%%%%%%%%%%
% Get an image file
[fname,pathName] = uigetfile('*.*');
if isequal(fname,0)
    return
end
markerSpecs = getappdata(gca,'markerSpecs');
delete(gca)
initializeAxes([pathName,fname],markerSpecs)




function callback_loadPoints(varargin)
```

```
%%%%%%%%%%%%%%%%%%%%%%%%%
% Check if an image has been loaded
if ~isempty(findobj(gca,'type','text'))
    errordlg('Please load an image before loading
points.','Error')
    return
end
%%%%%%%%%%%%%%%%%%%%%%%%%
% Check if there are existing points
if ~isempty(getappdata(gca,'H'))
    button = questdlg(['Loading new points will clear current
points.  ',...
        'OK to continue?'],'Warning!!','OK','Cancel','OK');
    if isequal(button,'Cancel')
        return
    end
end
%%%%%%%%%%%%%%%%%%%%%%%%%
% Get a points file
[fname,pathName] = uigetfile({'*.dat','Data files (*.dat)';
'*.mat','MAT files (*.mat)'});
if isequal(fname,0)
    return
end
%%%%%%%%%%%%%%%%%%%%%%%%%
% Check that the data are in the correct format
ext = fname(end-3:end);
switch ext
    case '.dat'
        XY = load([pathName,fname]);
        if size(XY,2)~=2
            errordlg('Data must be an m-by-2
matrix.','Error')
            return
        end
    case '.mat'
        w = whos('-file',[pathName fname]);
        if length({w(:).name})>1
            errordlg('.mat file must contain only one
variable.','Error')
            return
        elseif w.size(2)~=2 || length(w.size)~=2
            errordlg('Data must be an m-by-2 matrix','Error')
            return
        else load([pathName,fname])
```

```
            eval(['XY = ',w.name,';'])
        end
    otherwise
        errordlg('Must only load .dat or .mat
files.','Error')
        return
end
%%%%%%%%%%%%%%%%%%%%%%%%
%Check that the data fall within the axes boundaries
axlim = getappdata(gca,'axlim');
if min(XY(:,1)) < axlim(1) ||...
        max(XY(:,1)) > axlim(2) ||...
        min(XY(:,2)) < axlim(3) ||...
        max(XY(:,2)) > axlim(4)
    errordlg('Loaded points must be inside axes
boundaries.','Error')
    return
end
%%%%%%%%%%%%%%%%%%%%%%%%
%Delete old data:
delete(getappdata(gca,'H'))
%%%%%%%%%%%%%%%%%%%%%%%%
%Plot new data
H = d07_plotPoints(XY);
setappdata(gca,'H',H)
```

```
function callback_export2Base(varargin)
%%%%%%%%%%%%%%%%%%%%%%%%
[XY] = getXY;
if isempty(XY)
    msgbox('No existing points.  Please digitize at least one
point before exporting.',...
        'Warning!','warn')
else
    assignin('base','XY',XY)
    msgbox('Data exported to Workspace.  Variable name:
''XY''')
end
```

```
function callback_export2File(varargin)
%%%%%%%%%%%%%%%%%%%%%%%%%
% Check for existing points
[XY] = getXY;
if isempty(XY)
    msgbox('No existing points.  Please digitize at least one
point before exporting.',...
        'Warning!','warn')
    return
end
%%%%%%%%%%%%%%%%%%%%%%%%%
% Get a file name for writing
ext = varargin{3};
[fname,pathname] = uiputfile({['*',ext],[upper(ext(2:4)),'
Files (',ext,')']});
if isequal(fname,0)
    return
end
%%%%%%%%%%%%%%%%%%%%%%%%%
% Check the file extension of the chosen file
if ~isempty(findstr('.',fname))
    ext = fname(end-3:end);
    if ~ismember(ext,{'.dat','.mat'})
        %the user has chosen a different file extension
        errordlg('Please use the default extension.','Error')
        return
    end
end
%%%%%%%%%%%%%%%%%%%%%%%%%
% Write data
switch ext
    case '.mat'
        save([pathname,fname],'XY')
        msgbox('Data exported.  Variable name: ''XY''')
    case '.dat'
        if isempty(findstr('.',fname))
            fname = [fname,'.dat'];
        end
        save([pathname,fname],'XY','-double','-ascii','-
tabs')
```

```
        msgbox('Data exported.')
    otherwise

end
```

```
function callback_changeStaticColor(varargin)
%%%%%%%%%%%%%%%%%%%%%%%%
markerSpecs = getappdata(gca,'markerSpecs');
c = uisetcolor(markerSpecs.statColor,'Choose Marker Color');
if ~isequal(c,0)
    markerSpecs.statColor = c;
    set(getappdata(gca,'H'),'color',c)
    setappdata(gca,'markerSpecs',markerSpecs)
end
```

```
function callback_changeDragColor(varargin)
%%%%%%%%%%%%%%%%%%%%%%%%
markerSpecs = getappdata(gca,'markerSpecs');
c = uisetcolor(markerSpecs.dragColor,'Choose Marker Color');
if ~isequal(c,0)
    markerSpecs.dragColor = c;
    setappdata(gca,'markerSpecs',markerSpecs)
end
```

```
function callback_changeMarkerSize(varargin)
%%%%%%%%%%%%%%%%%%%%%%%%
markerSpecs = getappdata(gca,'markerSpecs');
a = inputdlg({'Enter marker
size:'},'',1,{num2str(markerSpecs.size)});
if ~isempty(a)
```

```
    a = str2double(a{1});
    try
        H = getappdata(gca,'H');
        set(H,'markersize',a)
        markerSpecs.size = a;
        setappdata(gca,'markerSpecs',markerSpecs)
    catch
        err = lasterror;
        errordlg(err.message,'Marker Size Error')
        return
    end
end
```

```
function callback_changeSymbol(varargin)
%%%%%%%%%%%%%%%%%%%%%%%%%
symbol = varargin{3};
H = getappdata(gca,'H');
set(H,'marker',symbol)
markerSpecs = getappdata(gca,'markerSpecs');
markerSpecs.style = symbol;
setappdata(gca,'markerSpecs',markerSpecs)
```

```
function deletePoint(varargin)
%%%%%%%%%%%%%%%%%%%%%%%%
h = varargin{3};
H = getappdata(gca,'H');
H(H==h)=[];
setappdata(gca,'H',H)
delete(h)
```

```
function deleteAllPoints(varargin)
```

```
%%%%%%%%%%%%%%%%%%%%%%%%
button = questdlg('OK to delete all
points?','Warning!!','OK','Cancel','OK');
if isequal(button,'Cancel')
    return
end
delete(getappdata(gca,'H'))
setappdata(gca,'H',[])
```

```
function closeFigure(varargin)
%%%%%%%%%%%%%%%%%%%%%%%%
button = questdlg('Export data to Workspace before
closing?',...
    '','Export&Close','Close','Cancel','Export&Close');
switch button
    case 'Export&Close'
        [XY] = getXY;
        assignin('base','XY',XY)
        fprintf('\n\nData imported from Digitize2D:\n')
        fprintf('   Name: ''XY''\n')
        fprintf('   Size: [%.0f %.0f]\n\n',size(XY))
        delete(gcf)
    case 'Close'
        delete(gcf)
    case 'Cancel'
        return
end
```

```
%% UTILITY FUNCTIONS


function [XY] = getXY
```

```
H = getappdata(gca,'H');
XY = [get(H,'xdata') get(H,'ydata')];
if length(H)>1
    XY = cell2mat(XY);
end
```

Avd för Teknisk Vattenresurslära
TVVR-YY/500n
ISSN 1101-9824

Wave-Damping Properties Of Swimming Lines

Nadim-Pierre Rizk